IMSE

Institute for Materials Science and Engineering

NONDESTRUCTIVE EVALUATION

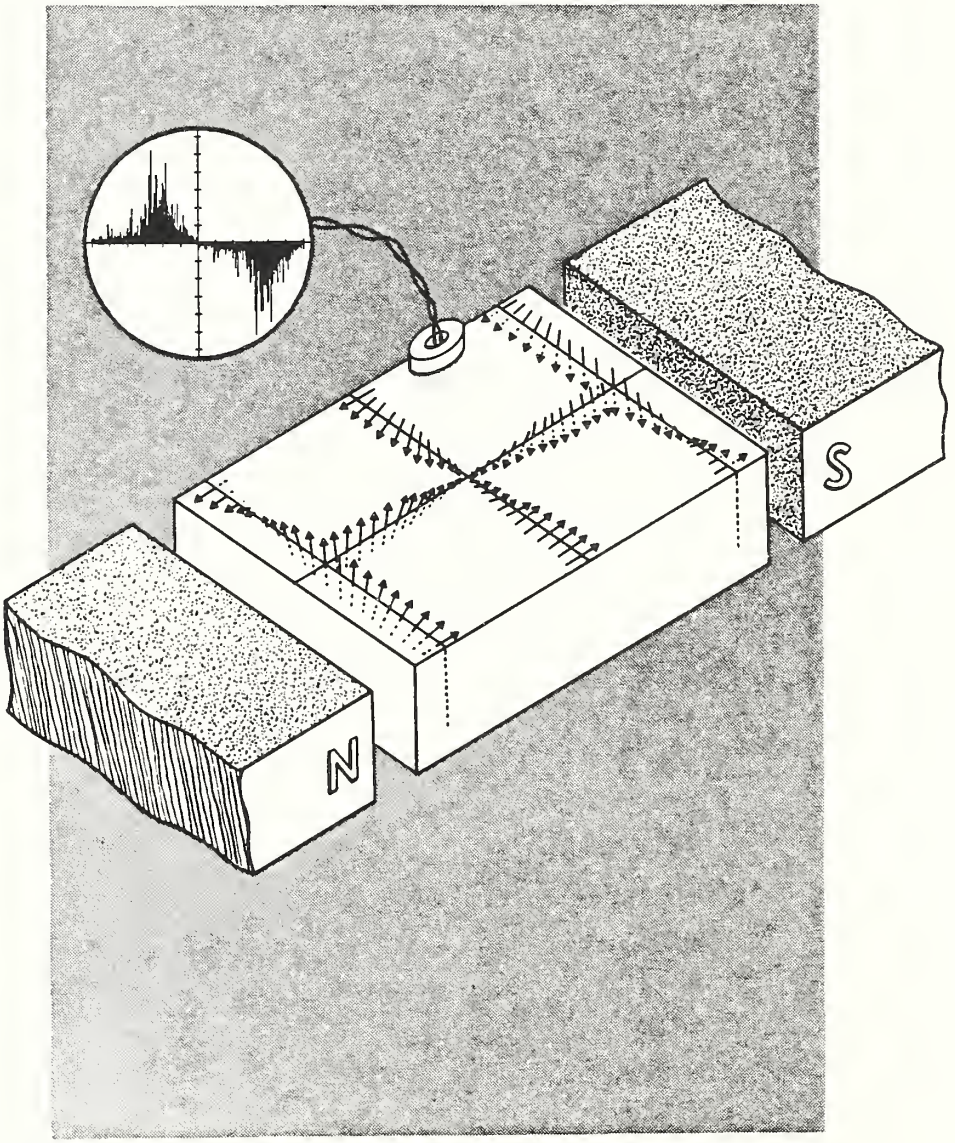

NAS-NRC
Assessment Panel
February 1–2, 1990

NISTIR 89-4147
U.S. Department of Commerce
National Institute of Standards
and Technology

Technical Activities 1989

Discontinuous motion of domains in a magnetic material result in Barkhausen noise. Characteristics of this noise are related to the material's microstructure and stress state.

IMSE

Institute for Materials Science and Engineering

NONDESTRUCTIVE EVALUATION

H. Thomas Yolken, Chief
Leonard Mordfin, Deputy Chief

NAS-NRC
Assessment Panel
November 1989

NISTIR 89-4147
U.S. Department of Commerce
National Institute of Standards
and Technology

Technical Activities 1989

Certain commercial equipment, instruments, or materials are identified in this report in order to adequately specify the experimental procedure. In no case does such identification imply recommendation or endorsement by the National Institute of Standards and Technology, nor does it imply that the materials or equipment identified is necessarily the best available for the purpose.

TABLE OF CONTENTS

INTRODUCTION

Fiscal year 1989 marked the sixth year of definite progress towards reaching many of the objectives and goals as stated in our December 1984 Strategic Plan. This Plan changed the major direction of the program to NDE for process control from NDE for in-service inspection.

Fiscal year 1989 also saw the useful dialogue from two industrial workshops serve as additional information for our new strategic plan that was developed last year. This plan, which should be viable well into the 1990's, involves a proposed major expansion of our activities into the broader arena of intelligent processing of materials.

Our research efforts were focused this year, as they were the previous year on four selected high-priority activities: NDE for Ceramic and Metal Powder Production and Consolidation, NDE for Formability of Metals, NDE for Composites Processing and Interfaces, and NDE Standards and Methods. This focused approach provides enhanced synergism between our NDE research efforts and NIST efforts in materials science and engineering, and provides greater interactions with industry.

The researchers working on the NIST NDE Program have made a number of significant scientific and technical advances. Although this report contains descriptions of these advances, I would like to highlight a few of the more significant of these.

An industrial consortium, consisting of Crucible Materials, Hoeganaes, and General Electric, working with NIST, has successfully completed the second year of a three-year program to develop intelligent processing technology for rapidly solidified metal powders. The NIST principal investigators are Steve Ridder and Frank Biancaniello of the Metallurgy Division; George Mattingly, Cary Presser, Pedro Espina, and Serge Huzarewicz of the Center for Chemical Engineering; and Steve Osella and Ted Hopp of the Center for Manufacturing Engineering. Progress continued towards developing a fundamental understanding of the liquid jet break-up leading to metal droplet formation. This understanding was based on utilizing a variety of in situ measurement techniques such as Schlieren and high speed photography, optical holography, and pressure surveys along with fluid dynamics modeling techniques. Research also moved ahead in applying in situ particle sizing techniques to determine droplet size. In addition, progress was made on designing and implementing the intelligent control system, which included acquisition of needed hardware and development of software.

Noteworthy advances were again made in the joint effort between The Aluminum Association and NIST to develop an internal temperature distribution sensor for monitoring the extrusion of aluminum. Arnold Kahn of the Metallurgy Division and Mike Mester from The Aluminum Association have utilized flat eddy current coils and data handling techniques to extend their temperature sensing technique to thin, flat sections such as U-channels, I-beams, and flat strips and sheets. A system has been designed and was demonstrated in in-plant testing.

A barrier to the implementation of advanced polymer composites in many applications is that the processing lacks the desired reliability. A. J. Bur, A. Lee, R. E. Lowry, S. C. Roth, F. W. Wang, and coworkers of the Polymers Division have greatly extended their fluorescence spectroscopy technique for on-line monitoring of polymer processing. They showed that the NDE technique can be used to monitor polymer shear stress, non-Newtonian viscosity, flow instabilities, etc. of polymer melts during processing.

ONDE continued to provide leadership in the development and promulgation of documentary standards for NDE. Work on real-time radiography and thermography are two of the several areas where good progress has been made.

The prospects look bright for our Program over the next few years in both our traditional role of NDE sensors and standards and in our new thrust area involving the intelligent processing of materials.

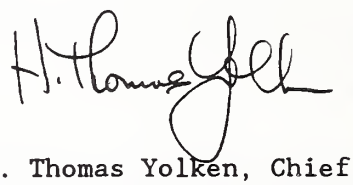

H. Thomas Yolken, Chief
Office of Nondestructive Evaluation

TECHNICAL ACTIVITIES

A. NDE FOR CERAMIC AND METAL POWDER PRODUCTION AND CONSOLIDATION

This activity is mainly concerned with developing approaches, sensors, and procedures for nondestructively determining those properties of ceramic and metal powders, and of consolidated materials, that relate to the quality and performance of the materials and manufactured parts. The emphasis is primarily on measurements that can be made during the manufacturing process to sense the pertinent properties of the product during critical stages of its formation and to provide the data required to control the process. The activity includes development of sensors for metal powder atomization systems, characterization of compacted and sintered ceramics by measurements of the complex dielectric constant, and determination of machining damage by thermal waves. The project on metal powders is aimed at developing an intelligent processing system and involves the development of a process model, the investigation of a variety of sensors and their performance in an actual inert gas/metal atomization facility, and an expert system for the process control. This project is viewed as a model system to obtain experience and insight on how to approach the complete problem of process sensing and control. Representative accomplishments in this activity during the past year include:

- In the program on the metal atomization system, progress was made toward (a) an understanding of the liquid jet break-up leading to droplet formation and the development of a process model, (b) real-time methods for in situ sensing of droplet size distribution and velocity, and (c) development of an intelligent control system.

  (a) Several flow measurement techniques were used to study the salient features of the gas-only flow. Recent studies included the off-axis characteristics of the static pressure and velocity distributions. Also studies of the effect of various process parameters on the resulting particle size distribution were completed. These data will be used in developing the process model.

  (b) Particle sizing techniques were studied for diagnostics in the spray formation region and the exit exhaust stream. A line-of-sight instrument using Fraunhofer diffraction was used to obtain measurements of mean particle size in the atomizer exit section. A comparative evaluation of several techniques was performed for particle sizing in small volumes in the spray formation region downstream of the atomizing die. The results indicated which of the techniques are more sensitive to smaller particle-size range and which are more sensitive to larger particle-size range.

  (c) Recent efforts were focused on preparations for the new data acquisition and control system. Work continued on the intelligent control system (ICS) software based on simulations of the atomization process. Critical to the ICS's ability to control the atomization process is the acquisition of particle size information from the Fraunhofer diffraction particle sizing instrument. These data will be used by the ICS in determining the quality of the processed powder, by a learned knowledge data base, to provide the response to particle size changes necessary for process control.

- In the program on the NDE characterization of ceramic sintering, alumina specimens were prepared including a glass-containing sample to represent a second phase content of sintered alumina samples. The samples were isostatically pressed to eliminate density variations in the green state and sintering was carried out to obtain densities between 95% and 99.5% of the theoretical density. The complex dielectric constant, which was obtained as a function of frequency by time domain spectroscopy, was found to be a sensitive indicator of changes in porosity (densification) and second phase (glass) content of sintered alumina specimens. The measured dispersion (variation of complex dielectric constant with frequency) was clearly due to interfacial polarization. A very broad dispersion seen in the glass-containing sample is indicative of multiple dielectric relaxation processes.

- An investigation of machining damage in ceramics with the mirage thermal wave method was continued. The samples (hot pressed Si_3N_4 cutting tool specimens from the Norton Company) were polished to a diamond finish and then subsequently ground to coarser and coarser surfaces. After each grinding treatment, the thermal diffusivity, α, was measured as a function of frequency. It was found that the frequency behavior of α, which reflects the bulk value and that of the surface damage due to the grinding, correlated with the coarseness of the grinding and reflected the presence of the damaged surface layer. Because the measured values of α are quantitative and reproducible, in principle they could be used to quantify the residual damage from grinding.

Intelligent Processing of Rapidly Solidified Metal Powders

S. D. Ridder and F. S. Biancaniello
Metallurgy Division
Institute for Materials Science and Engineering

G. E. Mattingly and P. I. Espina
Chemical Process Metrology Division
Center for Chemical Engineering

C. Presser, S. Huzarewicz and H. G. Semerjian
Chemical Process Metrology Division
Center for Chemical Engineering

T. Hopp and S. A. Osella
Factory Automation Systems Division
Center for Manufacturing Engineering

Metal powders less than 45 μm in diameter were shown to have unique properties due to their chemical homogeneity, metastable phases, and/or other novel microstructural features.[1,2] The primary factor that determines these features is solidification rate, which for powder processing depends on the amount of undercooling (which is inversely related to particle size) achieved by the metal droplets prior to solidification. This strong dependence of properties on solidification rate translates into an increased demand on the process engineer to control particle size. Fortunately, gas atomization has the necessary

flexibility within its process parameters to allow powder size control once particular characteristics of the system are understood.

The research reported here is aimed at developing an instrumentation system that is capable of monitoring and controlling the atomization process parameters to achieve the desired particle size distribution. This system would operate in real time using inputs from process sensors (for temperatures, pressures, particle size, etc.) and outputs to process actuators in a feedback-loop controller based on an expert system. The approach taken to realize this goal is to develop: (1) a fundamental understanding of liquid jet breakup processes that lead to droplet formation, (2) real-time sensing techniques for in-situ measurement of droplet/particle size distribution, and (3) expert systems for control of the atomization process using process models developed in (1) and particle sensing techniques in (2).

(1) Process and Model -- Efforts have continued to study droplet formation mechanisms within the specific "consortium" atomization die (see refs. 2, 3, 4, or 5 for schematic drawings). This die produces a circle of supersonic gas jets that impinge on a central, downward flowing, molten metal stream that is aspirated through the delivery nozzle. Detailed characteristics of the supersonic gas flow are critical in determining the nature of the liquid stream break-up and the size of the metal droplets formed. The research strategy adopted to produce the desired understanding of these flow processes is to begin with the gas-only flow and continually change conditions and parameters to progress toward the more harsh and hostile conditions present in the actual atomization process.

A range of flow measurement techniques were used to measure and understand the salient features of the gas-only flow. Schlieren photography, pressure and temperature surveys, and optical holography were previously reported.[3-5] Initial pressure surveys along the axis of symmetry of the gas-only flow showed quantitatively the flow characteristics produced via the visualization techniques. More recently, these surveys were expanded to include the off-axis characteristics. Data values were acquired at 160 co-planar positions within the gas-only flow from three different probes (static pressure, stagnation pressure and stagnation temperature). These data were used to calculate the spatially resolved velocity profiles for four operating pressures. Typical results are shown in Figures 1 and 2. The static pressures are normalized to atmospheric pressure, P_r, and velocities are normalized using $V_{max} \equiv$ maximum measured velocity = 420 meters per second. When the liquid stream is present, these distributions are altered because of the interactions which occur at, and downstream of, the gas-liquid contact point. Upstream of this contact point in the actual atomization process, the gas flow should closely resemble that occurring in the gas-only flow.

This gas flow upstream of the contact point can be analyzed using the Method of Characteristics which is a set of procedures that can be used to compute certain gas flows.[6] This technique was applied to gas expansion from a die and gas jet geometry that is intended to approximate that of our selected shape. The approximation is that of a two-dimensional die in which the delivery tube outlet is a slot and the gas exits not from a ring of discrete holes but rather from a slot that parallels the delivery tube outlet. Results of this analysis

were included in refs. 4 and 6. It is planned that this method will be used to compute gas-only flows for other die pressure conditions of interest.

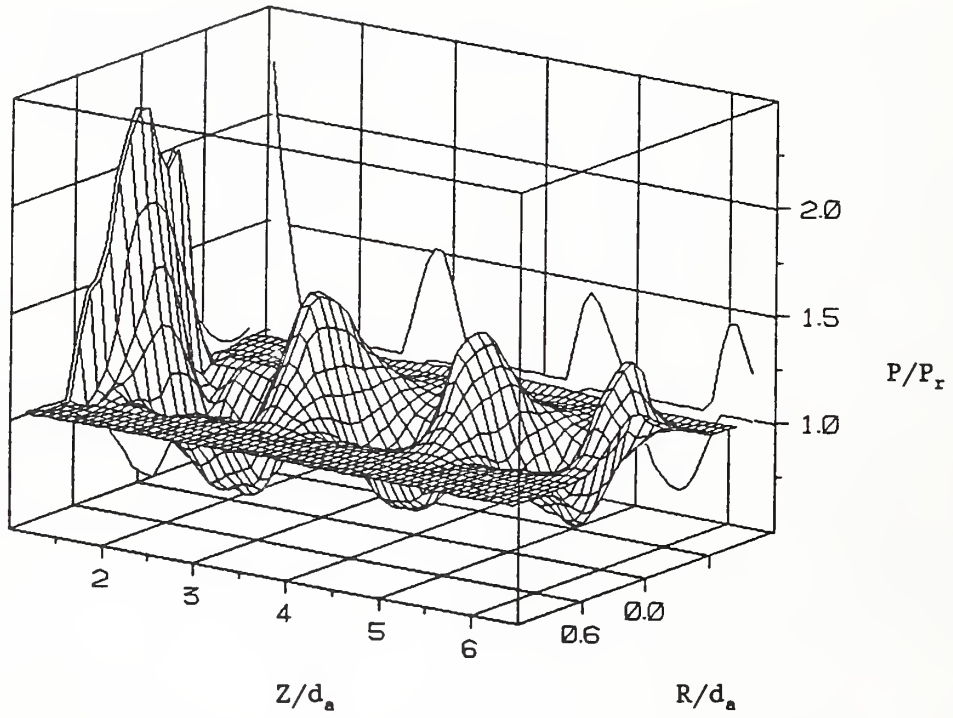

Figure 1. Three dimensional surface showing dimensionless static pressure, P/P_r, in gas-only flow at the optimal die pressure condition. P is static pressure, P_r is atmospheric pressure, R is the radial coordinate position, Z is the axial coordinate position, and d_a is a characteristic jet diameter.

The current thrust of the metallurgical processing subgroup is the completion of a parameterization study. This involves a series of atomization runs where appropriate process parameters are identified and changed in a systematic way to quantify each parameter's effect on the resulting particle size distribution. During each atomization run a different parameter (atomizing gas pressure, metal flow rate, or metal temperature) is changed and the powder is collected. Particle size distributions for each of these atomization runs is subsequently determined via mechanical sieve analysis. Runs completed to date include combinations of three different pressures and two melt temperatures (six different atomizing conditions) with at least one repeat for data confirmation. Additional experiments are scheduled for one more melt temperature at each of the three different pressures and then these nine combinations will be run again at a different metal flow rate (18 different conditions in all). When completed these data will be used in developing the atomization controller and for comparison with the in situ particle size sensor.

High-speed movies (10,000 fps) made during most of the parameterization study experiments were used to study fragmentation mechanisms. Spatial resolution was increased to the several hundred μm range by utilizing special magnifying optics and high resolution film. Results of frame-by-frame digital image enhancement were used to determine the primary droplet formation mechanisms

(see refs. 5 and 6 for detailed description). These movies clearly show the initial liquid metal sheet being pulled from the edge of the molten metal delivery tube and the subsequent ligament and primary droplet formation from this sheet. The primary droplets are seen to recirculate (on occasion for several cycles) and/or undergo secondary break-up into finer droplets before entering the high-speed gas flow and accelerating to speeds beyond the temporal resolution limit (200 m/s).

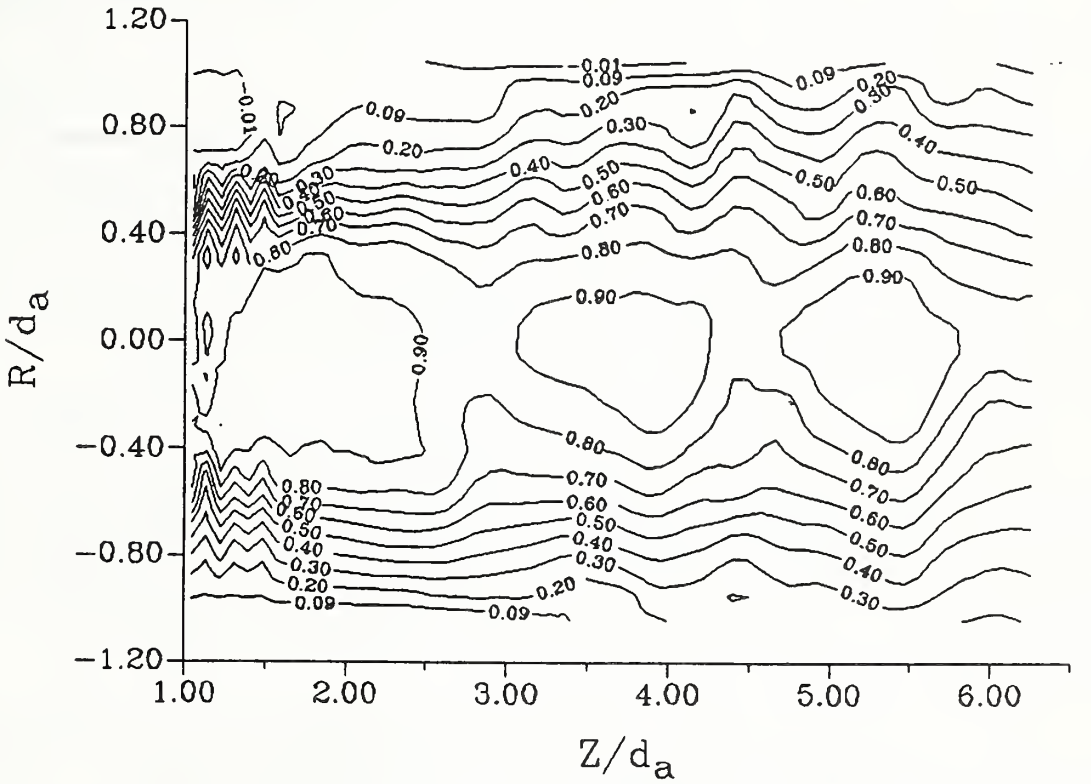

Figure 2. Two-dimensional contour plot of dimensionless velocity distributions, V/V_{max}, in gas-only flow at the optimal die pressure condition where V is gas velocity and V_{max} is the maximum measured velocity = 420 m/s. R, Z, and d_a are the same as in Figure 1.

(2) Sensors -- Particle sizing techniques are being studied for diagnostics in two sections of the inert gas atomizer facility; viz., (a) in the spray formation region downstream of the atomizing die, and (b) in the exhaust stream of the atomizer exit section. A comparative evaluation of three point-measurement techniques was performed in previous measurements in liquid sprays; these include (a) polarization ratio, (b) scattered light intensity deconvolution (LID), and (c) phase/Doppler interferometric (PDI) techniques. Results indicated that the first two techniques are more sensitive to the smaller particle size range ($d < 5\ \mu m$), whereas the third one provides more reliable measurements for larger droplets ($d > 3\mu m$).[7] Experiments are currently being carried out with the PDI instrument.

A line-of-sight measurement technique was selected to obtain a representative measurement of particle mean size in the atomizer exit section. The instrument

operates on the principle of Fraunhofer diffraction, in which particles diffract laser light onto a calibrated multi-element ring diode.[8,9] The particle size distribution, averaged along a cross section of the process stream, can then be used to determine particle mean size and other statistical properties. The instrument provides good time resolution for the high process flow rates ($\simeq$ 1 m/s) and short run times encountered during atomization (typically 2 min.).

To date, measurements were carried out successfully with the laser diffraction device during several metal atomization runs. The particle size distribution was found to be multi-modal and included a wide range of particle sizes (i.e., $7 < d < 150$ μm). The particle mean size also turned out to be relatively constant during each run. High obscuration levels (approximately 60%) measured during these runs indicated that the metal powder stream passing through the exhaust section contained a high concentration of particles. The effects of Schlieren induced beam steering (possibly due to temperature gradients) was also considered in the analysis of the raw data. This beam steering effect was indicated by the presence of an anomalous peak in the particle size distribution at a volumetric median diameter of approximately 250 μm. (Beam steering could also affect the obscuration level measurement previously mentioned.) A detailed discussion of these results was presented in refs. 8 and 9.

Future activities will include continued operation of the laser diffraction system in both the exit section of the atomizer and in an off-line continuous powder flow facility recently procured. The off-line experiments will allow indefinite run times on predetermined particle size distributions and should provide a good test system to evaluate the particle sensors' problems and capabilities. The PDI and LID sizing devices will be available to obtain data in the metal atomizer, the off-line powder feeder, and the gas diagnostics/ surrogate fluid atomizer.

(3) Intelligent Control System -- Current efforts are focused on necessary preparations for the new Data Acquisition and Control (DAC) system. The DAC system was determined to be vital to the integration of an advanced control system for the atomization process. These preparations included the construction and installation of a digital I/O interface board, a micro-computer based DAC, and a low-voltage switchboard for manual control of the atomizer's process actuators. (This switchboard simplifies the implementation of automatic control by TTL-level signals from the computer.) A serial interface was installed for communication between the DAC and the Intelligent Control System (ICS).

Work continued on the ICS software based on simulations of the atomization process. The operator, via the user interface, can plan and execute atomization runs, monitor process conditions during runs, and analyze process data subsequent to the runs. The ICS is responsible for reconciling user requests with current process conditions in order to meet production objectives. The reconciliation will be accomplished via heuristic process control knowledge provided by the operator(s) as well as learned knowledge acquired inductively during atomization experiments. Details of the control system have been included in a recent publication.[10]

Critical to the ICS's ability to control the atomization process is the acquisition of particle size information. The Fraunhofer Diffraction Particle

Sizing Instrument (FDPSI) provides both raw detector values and detailed calculations of size distribution (see discussion in section (2) above). However, transmission of this information is currently hindered by software imposed restraints. New software will be installed in the FDPSI that will allow remote access to the detector values via serial communication with the ICS. These raw detector values will be used by the ICS in determining the quality of the process powder by a learned knowledge data base. This technique will provide the "rapid" response (above 1 Hz) to particle size changes necessary for process control.

References

1. W. J. Boettinger, L. Bendersky, and J. G. Early, "An Analysis of the Microstructure of Rapidly Solidified Al-8 Wt Pct Fe Powder," Metall. Trans. A 17 (1986), pp. 781-790.

2. S. D. Ridder and F. S. Biancaniello, "Process Control During High Pressure Atomization," Mat. Sci. Eng. 98, 47-51 (1988).

3. P. I. Espina, et al., "Aerodynamic Analysis of the Aspiration Phenomena in a Close-Coupled Inert Gas Atomizer" (presented at the 118th TMS Annual Meeting, Las Vegas, Nevada, 28 February 1989).

4. S. D. Ridder, F. S. Biancaniello, and P. I. Espina, "Laser Holographic Imaging of the Two Fluid Atomization Process" (presented at the 118th TMS Annual Meeting, Las Vegas, Nevada, 28 February 1989).

5. S. D. Ridder, P. I. Espina, and F. S. Biancaniello, "Optimization of Inert Gas Atomization" (to be presented at the TMS-sponsored Symposium-Physical Chemistry of Powder Metals Production and Processing to be held in St. Marys, PA, on October 16-18, 1989.

6. A. H. Shapiro, The Dynamics and Thermodynamics of Compressible Fluid Flow, (New York, NY: John Wiley & Sons, 1953).

7. C. Presser, et al., "Laser Diagnostics for Characterization of Fuel Sprays," Proc. 5th Intl. Congress on Appl. of Lasers and Electro-Optics (ICALEO 1986) 58, 160-167 (1986).

8. F. S. Biancaniello, C. Presser, and S. D. Ridder, "Real-Time Particle Size Analysis During Inert Gas Atomization" (presented at the TMS-AIME Fall Meeting, Chicago, IL, 1988).

9. C. Presser, et al., Laser Diffraction Measurements in an Inert-Gas Metal Atomizer" (presented at the 3rd Annual Conference on Liquid Atomization and Spray Systems ILASS-Americas, Irvine, CA, 1989).

10. S. A. Osella, "Collective Learning Systems: A Model For Automatic Control," (presented at IEEE Intelligent Control Symposia, Albany, NY, 1989).

Nondestructive Characterization of Ceramic Sintering

J. E. Blendell and J. F. Kelly
Ceramics Division
Institute for Materials Science and Engineering

F. I. Mopsik
Polymers Division
Institute for Materials Science and Engineering

This study demonstrates that dielectric spectroscopy can be used to nondestructively assess the microstructural state of alumina ceramics. The dielectric dispersion is determined to be a sensitive indicator of changes in porosity and second phase (glass) content of sintered alumina specimens. The nature of the observed dispersion curves are shown to be consistent with the simple grain-grain boundary structure for the pure aluminas and a multi-interface structure for the glass doped aluminas.

The determination of these fundamental material electrical characteristics are necessary for the development of an on-line, non-contacting probe to measure the dielectric response during sintering. Such a probe would be used as part of an intelligent processing system to control the sintering conditions necessary to reproducibly obtain a specific microstructure.

A. Sample Preparation and Characterization

Sintering of ceramics involves the removal of porosity and, at later stages, grain growth. Because grain boundary energy is less than half that of a free surface, initially the system energy is lowered by increasing the area of contact of the grains from point contacts to finite areas. This leads directly to a reduction of porosity. When the pore size is small enough, usually at porosities of less than 10 percent, a further reduction in energy can occur by grain boundary movement and with a growth in grain size. While this later stage is occurring, there is a still further reduction in porosity.

Alumina samples were prepared under Class 100 clean room conditions. For the glass-containing samples, 4 weight percent anorthite ($CaO \cdot Al_2O_3 \cdot 2SiO_2$) was added to the alumina powder. Samples were isostatically pressed to eliminate density variations in the green state. The time-temperature conditions required for the desired densities were determined by sintering a sample of each composition in a dilatometer. Sintering was carried out in air between 1450°C and 1600°C. The densities obtained were between 95% and 99.5% of theoretical density.

B. Time-Domain Dielectric Spectroscopy

Three samples of alumina ceramic were measured; two pure alumina samples, sintered at 1450°C and 1600°C and another sample, containing 4% anorthite glass, was also sintered at 1600°C. The samples sintered at 1600°C are denser than that sintered at 1450°C. The capacitances were measured in a guarded disk geometry by time-domain spectroscopy for frequencies from 10^4 Hz to as low as 10^{-4} Hz. Measurement temperatures ranged from 50°C up to 175°C. The data were

analyzed in both the complex dielectric constant plane as well as the complex impedance plane.

The data in the complex impedance plane showed only a simple upswing at the lowest frequencies and will not be discussed in this report. The dielectric data did show a wide range of behavior and is very sensitive to the state of the sample as shown in Figure 1. Dielectric dispersion, variations of ϵ' with frequency, was observed for all the samples.

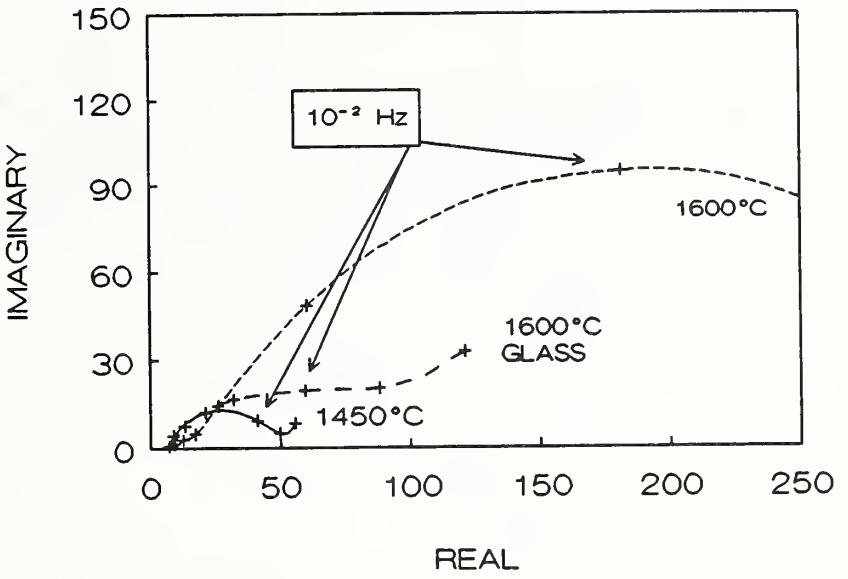

Figure 1. Real and imaginary components of the complex dielectric constant for alumina samples with and without glass additions and differing porosities. The crosses indicate the frequency decades decreasing left to right.

At 50°C, the two pure alumina samples showed a large change in ϵ' with densification. The less dense sample had a value for ϵ' of 6.8 at 1000 Hz while the more dense sample had an ϵ' of 9.9. Both ceramics showed two dispersion regions, one with a maximum above 10 kHz and the other near 10^{-3} Hz. The magnitude of the low frequency dispersion, however, was much larger for the dense sample, with a $\Delta\epsilon'$ of 10 while the less dense sample had a magnitude of 0.2. These values of $\Delta\epsilon'$ are indicative of a blocking layer that is much thinner for the denser sample. The sample containing glass, which had an ϵ' of 8.8 at 1 kHz, also showed two dispersion regions. The higher frequency dispersion was shifted to lower frequencies, with a maximum at 1 kHz, while the low frequency dispersion was unchanged from the pure alumina samples with an amplitude of 0.5. Both regions span a much broader frequency range than for the pure alumina samples.

At a measuring temperature of 175°C these differences persisted and became even stronger. The low frequency dispersion maximum shifted to 10^{-2} Hz, 6×10^{-2} Hz and 10^{-1} Hz respectively for the 1600°C and 1450°C pure alumina samples and the 1600°C alumina-with-glass sample, respectively. The dispersion amplitudes, $\Delta\epsilon'$, were 300, 40 and 70 for the two pure alumina samples and the glass-containing sample. The sample with glass showed much broader dispersions than the

two alumina samples. All the samples showed the beginning of a new loss region at 10^{-4} Hz.

C. Summary and Conclusions

The dispersions at 175°C are clearly due to interfacial polarization. The $\Delta\epsilon'$ and frequency shift are indicative of a blocking layer that is much thinner for the dense 1600°C pure alumina sample than for either the 1450°C pure alumina or glass-containing samples. This interpretation is based on a two phase series model, assuming that the thicker phase is more conductive than the thin phase. For the glass containing sample, the broad dispersions are indicative of multiple dielectric relaxation processes. These are consistent with the increased number of different interfaces and phases present in the sample. As seen in Figure 2, these effects can clearly distinguish among the samples. Further interpretation of the data is awaiting measurements (in progress) on alumina samples, with and without glass, of differing densities, pure sapphire, pure anorthite glass and a commercial alumina ceramic. Current work will further define the density range and glass content over which this technique can be used to monitor the sintering behavior of alumina ceramics.

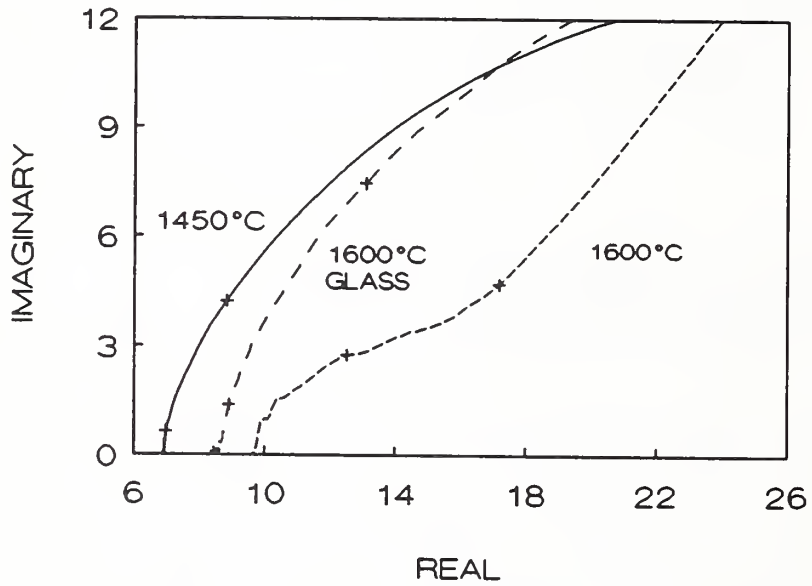

Figure 2. High frequency region of Figure 1. The changes in the high frequency dielectric constant with changes in the sample are clearly distinguishable.

Monitoring of Machined Ceramic Surfaces by Thermal Waves

G. S. White
Ceramics Division
Institute for Materials Science and Engineering

An investigation of machining damage in Si_3N_4 was continued with the mirage thermal wave measurement. (The term "thermal waves" is used to describe the

diffusion of heat in a material exposed to periodic surface heating. The thermal signal resulting from the periodic heating has the mathematical form of a critically damped traveling wave and is sensitive to variations in thermal properties of the material in much the same way that ultrasonic signals are sensitive to elastic property variations. The probe length for thermal wave measurements is μ, the thermal diffusion length, and depends on the period, or the modulation frequency, f, of the heating beam;

$$\mu = [\alpha/\pi f]^{1/2} \tag{1}$$

where α is the thermal diffusivity of the specimen.

In FY 1988, preliminary work on investigating machining damage in silicon nitride was conducted. Results of that work suggested that the thermal properties of the specimen surface were altered by the process of machining and that frequency profiles of thermal properties might detect these alterations as a function of depth into the specimen.

The central effort during FY 1989 consisted of measuring the thermal diffusivity of Si_3N_4 as a function both of f and of the degree of surface grinding. As inferred from Eq.(1), measurements at different frequencies provide values of α averaged over different depths into the specimen. The assumption tested was that, at lower frequencies, the measured value of α would be that of the bulk material but, at some higher frequency, the contribution from the altered thermal properties of the machining damaged layer would begin to be comparable to that of the bulk material and α would begin to change as a function of frequency. Implicit in this assumption was the idea that, at low enough frequencies, α would be insensitive to f and represent the true bulk value of thermal diffusivity in Si_3N_4. In practice, we found that for all grinding states of the specimen there existed a low frequency range for which α was insensitive to f, as expected, and above this frequency range α deviated from the low frequency value. However, we also found that the low frequency value of α depended upon the grinding state of the specimen and was particularly sensitive to coarse grinding.

Procedure and Results

Hot pressed Si_3N_4 cutting tool specimens from Norton Company were polished to a 6 μm diamond finish, providing a baseline for α measurements. Subsequent grinding steps included 9 and 15 μm diamond paste and 600 (22 μm), 400 (29 μm), and 320 (34 μm) grit SiC paper. After each grinding treatment, α was measured as a function of frequency using the mirage technique[2,3] in which the separation of the zero crossings of the in-phase component of the mirage signal, x, are related to the thermal diffusivity by

$$x = (1.4\alpha\pi/f)^{1/2} \tag{2}$$

Eq. 2 demonstrates that α can be determined from the slope, m, of the straight line fit to measurements of $(1/f)^{1/2}$ vs x:

$$\alpha = m^2/(1.4\pi) \tag{3}$$

Figure 1 shows the data corresponding to Eq. 2 for three surface treatments: 6 μm, 9 μm and 400 grit. The data from the 6 μm surface is linear over its entire range and corresponds to α = .22 cm^2/s. The 9 μm data deviate from linearity for f $\geq$ 965 Hz and those for 400 grit deviate from linearity for f $\geq$ 577 Hz. Figure 2 demonstrates that the frequency at which the data deviate from linearity, f_{dev}, correlates with the coarseness of the surface grinding, as predicted. However, we also found that, rather than being a true measure of the bulk value of α, at low frequencies, measured values of α depended on the surface treatment, particularly for coarsely ground surfaces. Figure 3 shows that, for fine grinding, the value of α is insensitive to surface treatment but, for coarse grinding, α begins to change noticeably.

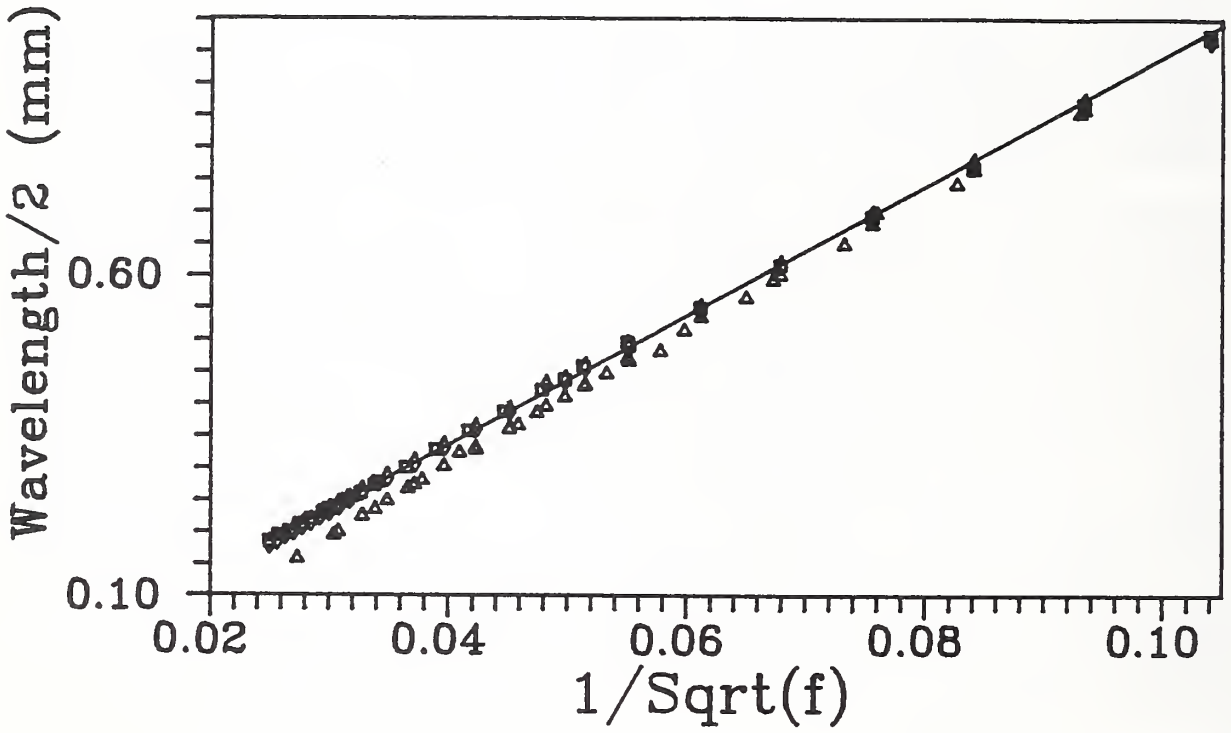

Figure 1. Plot of x vs $f^{-1/2}$ for Si_3N_4 polished through (Δ) 400 grit SiC paper, (◇) 9 μm diamond paste, and (□) 6 μm diamond paste. Solid line is a least square fit to the 6 μm data.

Both results, the deviation from linearity plotted in Figure 2 and the change in the low frequency measurements of α in Figure 3, correlate with the coarseness of grinding, reflecting the presence of the damage layer formed by the surface treatment. Because the measured values of α and f_{dev} are quantitative and reproducible, in principle, they could be used to quantify the residual damage from grinding.

Future Work

Future plans include a collaborative effort with the University of Dayton Research Institute (UDRI). They will prepare Si_3N_4 specimens with different surface treatments, and we will measure α as a function of frequency. UDRI

will subsequently fracture the specimens using standard fracture mechanics tests. A correlation between the strength of the specimens and the thermal wave signals will be made in an attempt to relate the frequency behavior of α to the surface treatment and, hopefully, the flaw population.

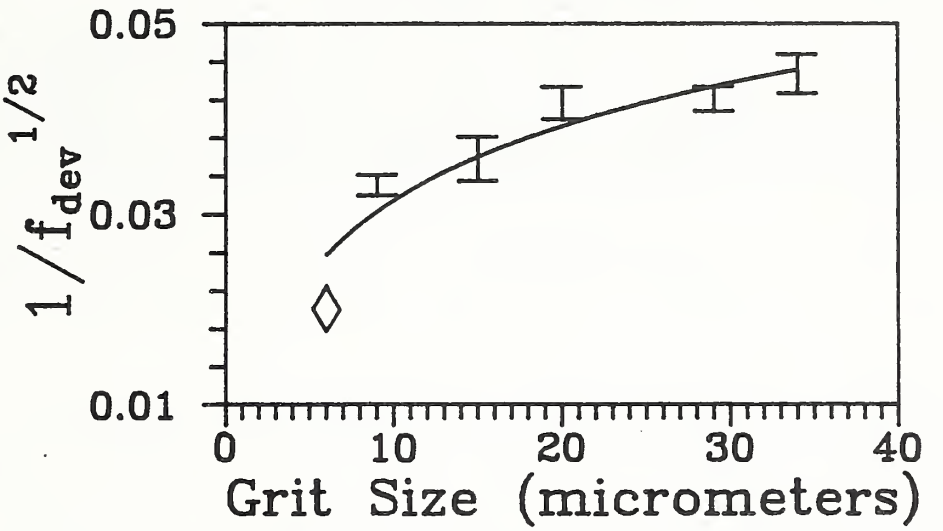

Figure 2. Plot of f_{dev} as a function of grinding grit size. Line is drawn to demonstrate trend of results but has no other significance.

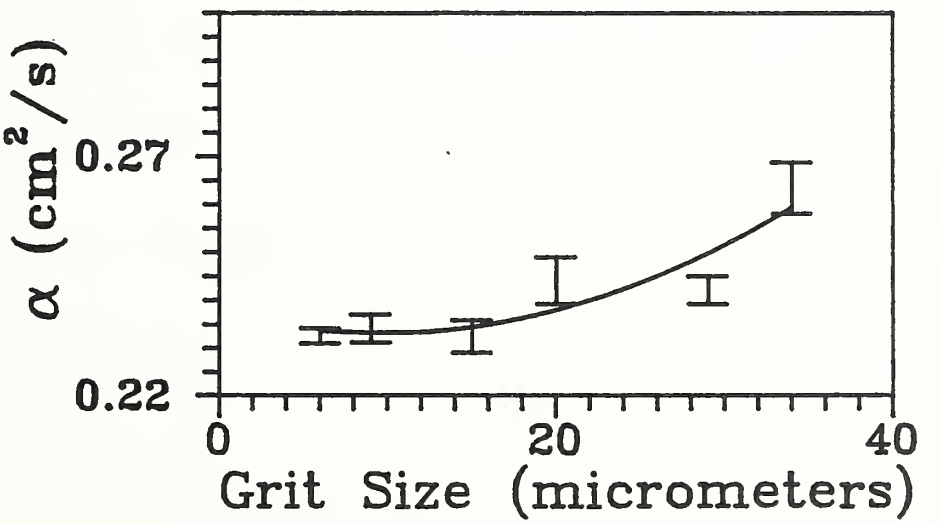

Figure 3. Plot of α vs grinding grit size. At coarse grinding, α determined by the mirage technique deviates from its bulk value.

References

1. G. Birnbaum and G. S. White, "Laser Techniques in NDE" in Research Techniques in Nondestructive Testing 7, ed. by R. S. Sharpe, pp. 259-365 (Academic Press, London 1984).

2. P. K. Kuo, M. J. Lin, C. B. Reyes, L. D. Favro, R. L. Thomas, D. S. Kim, Shu-Yi Hang, L. J. Inglehart, D. Fournier, A. C. Boccara, and N. Yacoubi, "Mirage Effect Measurement of Thermal Diffusivity. Part I: Experiment" Canadian J. Phys. 64, 1165-1167 (September 1986).

3. C. B. Reyes, J. Jaarinen, L. D. Favro, P. K. Kuo, and R. L. Thomas, "Reflection-Mirage Measurements of Thermal Diffusivity," in Review of Progress in Quantitative Nondestructive Evaluation 6 (D. O. Thompson and D. Chimenti, eds.), pp. 271-275 (Plenum Press, New York, NY 1987).

B. NDE FOR FORMABILITY OF METALS

The goal of this activity in the Nondestructive Evaluation Program is to develop generic approaches, sensors, and procedures for quantitative NDE of metals during the forming process. The emphasis is on measurements that can be made on the production line to improve process control rather than developing inspection techniques for post-manufacturing inspection.

Current efforts in this activity include: the development of NDE temperature sensors based on ultrasonic and eddy current techniques for determining the internal temperature distribution in hot metal objects, developing an in-process ultrasonic monitor for metal grain texture in manufacturing of sheet metal products, and utilizing ultrasonics for on-line monitoring of both metal surface roughness and cutting tool wear during machining. Examples of accomplishments this year include:

- During manufacture, the determination of internal temperature distribution in thin extruded aluminum sections for process control has been a troublesome problem for the aluminum industry. In a joint effort between NIST and The Aluminum Association, past years' theoretical and experimental results showed that a multifrequency eddy current measurement approach in the 100 kHz to 1 MHz range provided, for rounds and tubes, an NDE temperature sensor for process control. This year the approach was extended and applied to other shapes, such as I-beams.

- The formability of sheet metal, which in large part depends on grain texture or grain orientation, is a significant process variable in the manufacture of such diverse items as beverage cans, appliances, and automotive panels. In order to improve process control, a noncontacting ultrasonic method was developed over the past two years. This year's research in collaboration with Ford and the Advanced Steel Processing and Products Research Center demonstrated that the technique is applicable to thin ferritic steel sheet.

Eddy Current Temperature Sensing

A. H. Kahn
Metallurgy Division
Institute for Materials Science and Engineering

M. L. Mester
Research Associate
The Aluminum Association, Inc.

The joint NIST-Aluminum Association project on temperature measurement in extrusion processing had as its objective in 1988-89 the completion of the design and construction of a through-transmission sensor and its testing in a plant environment. These objectives have been met.

This sensor is based on the following principle of operation. Eddy currents are induced in the moving extrusion by ac driving currents in the transmitting coil. The signal received in the secondary coil is sensitive to the tempera-

ture dependent electrical conductivity of the extrusion, facilitating a temperature measurement. Calibration against a thermocouple was performed in the laboratory using samples of the extrusion product heated in a furnace and placed in the sensor.

The through-transmission sensor was installed in a canister that guided the extrusion in the press used for the tests. The assembly is shown in Figure 1. The primary coil is at the top; the secondary is located in the graphite web across the center. Both coils are water cooled. During production two aluminum I-beams were extruded simultaneously through the die of the press and passed into the canister, one each through the upper and lower sections. Temperature sensing was performed only on the upper extrusion.

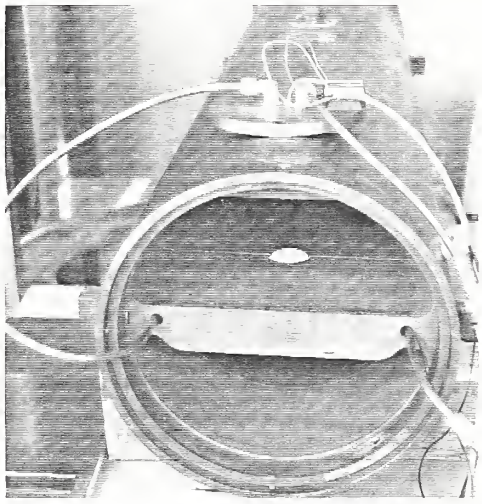

Figure 1. Through-transmission eddy current sensor installed in canister. Transmitter coil is at top; receiver coil is in the cental web.

Two plant tests were conducted at the R.D.Werner Company's plant in Greenville, PA. During these tests comparisons were made with measurements by radiometric methods and by the use of touch thermocouples held against the moving product. Each test was of approximately two hours duration. Aluminum I-beams were extruded at 160 ft/min. The temperatures measured by the eddy current system and the corresponding times were recorded by the controlling computer. Figure 2 shows a plot of typical data collected by the devices used; the Vanzetti radiometer, the Williamson radiometer, the touch thermocouple, and the eddy current sensor. The four sensors were calibrated to agree at 975°F on moving material.

The following characteristics are seen in Figure 2, which show the results on the complete passage of three billets. At the beginning of the extrusion of each billet the temperature was at a low value since the cool end of the billet was being extruded. (The billet had traveled in open air from the furnace to the press.) The extrusion temperature increased as the hot center of the billet was processed. In addition, the die temperature increased during the passage of the billet. The extrusion temperature reached a maximum at the end of the billet. At that point extrusion stopped, a new billet was introduced, and the process began again, with the new material welded to the old. Several features seen in Figure 2 are of special interest. When the end of a billet was reached the eddy current sensor showed an almost instantaneous drop of about 50°F. The apparent drop is caused by the termination of the motion and the

disappearance of the voltage induced by the motion of the product through the primary magnetic field. After the sudden drop, cooling of the stationary extrusion was observed. (During the stationary cooling the radiometric sensors did not collect data.) When the extrusion of the new billet began the separation between the old and new material presented a high resistance region to the eddy current sensor, which appeared as a fictitious "hot spot".

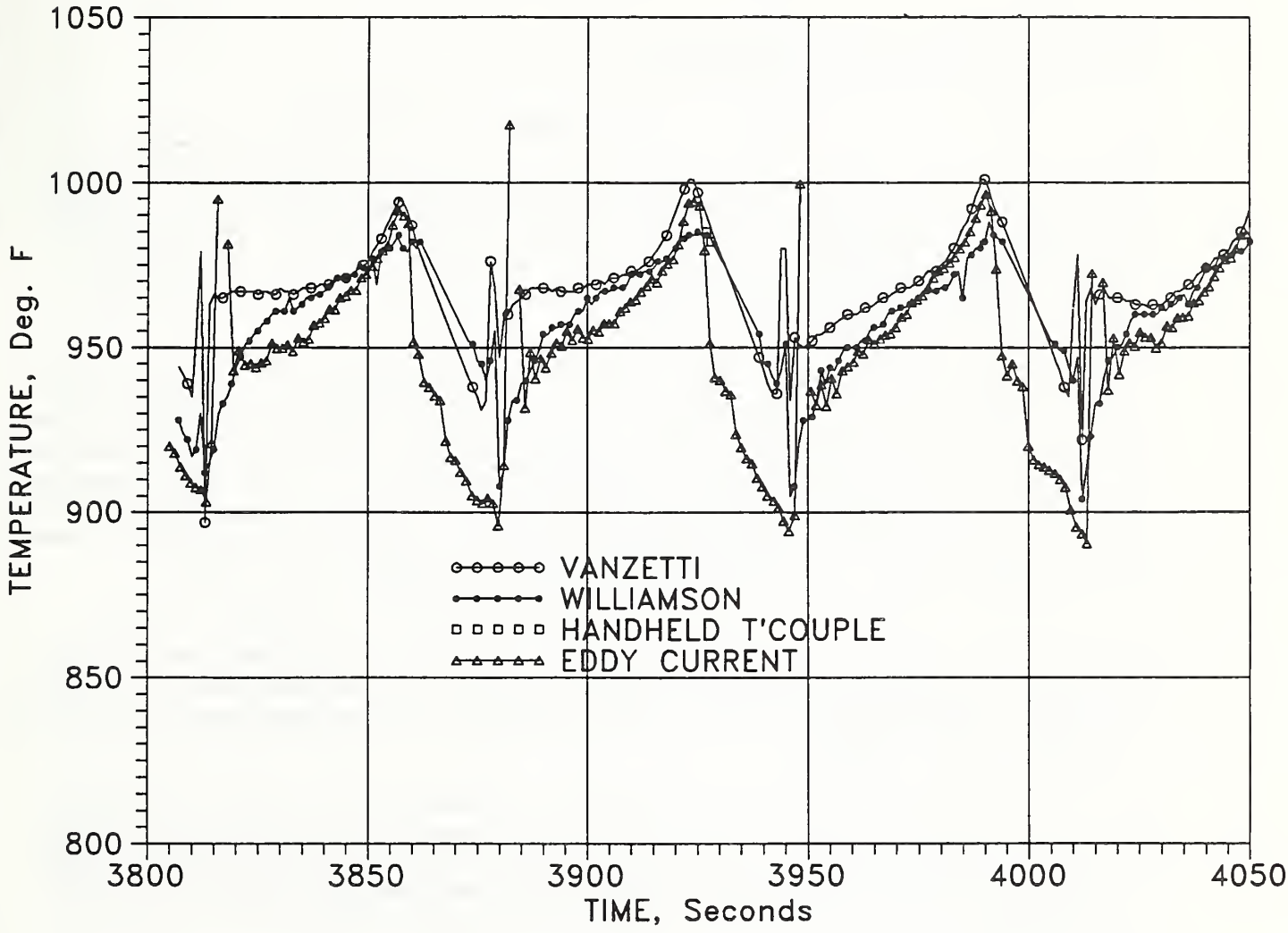

Figure 2. Typical temperature readings during extrusion test as recorded by the various sensor systems. Each repeated cycle corresponds to the extrusion of one billet.

The tests have demonstrated valuable comparisons between the different sensor types. The effect of velocity of the moving product on the temperature reading had not been taken into account. A theoretical calculation of this effect is now in progress. Disparities between the two types of radiometric measurements have not yet been reconciled.

Development of a Prototype Ultrasonic Instrument for Measurement of Sheet Metal Formability

A. V. Clark and D. V. Mitrakovic*
Fracture and Deformation Division
Institute for Materials Science and Engineering

G. V. Blessing
Automated Production Technology Division
Center for Manufacturing Engineering

*Guest Scientist from the University of Belgrade, Yugoslavia

Rolled steel sheet is used in many applications such as automobile body parts and household appliances. The formability of sheet has traditionally been measured by mechanical testing. Tensile specimens are cut at 0°, 45°, and 90° to sheet rolling direction and the strains in width and thickness directions, ϵ_w and ϵ_t, are measured for large plastic strains. The ratio, ϵ_w/ϵ_t, is the r-value, and is a commonly used industrial parameter.

It is known that the texture of the rolled sheet influences both formability and the elastic moduli. (Texture is the preferred orientation of the individual crystals that make up the sheet). Here, we seek a method for making ultrasonic velocity measurements and a correlation with r-values. In particular, we are using electromagnetic-acoustic transducers (EMATs) to generate and receive ultrasonic guided waves in the plane of the sheet. The noncontacting nature of these devices allows for velocity measurements to be made on moving sheet, and may ultimately lead to on-line formability measurements.

We have been collaborating with researchers at Ford Motor Company, who are independently making r-value measurements on sheet obtained from steel companies which are suppliers to Ford. The sheets, and the corresponding r-values, have been made available to us by Ford. We also obtained samples of sheet from a Japanese steel company.

We made ultrasonic measurements, using EMATs designed to generate and receive two types of guided waves in the sheet: the lowest-order symmetrical shear-horizontal (SH_0—) mode, and the lowest-order symmetrical Lamb-wave (S_0—) mode. The guided waves are predominantly transverse and longitudinal, respectively, for the plate thicknesses (about 1 mm) and frequency (500 kHz) in our experiments.

Velocity measurements were made for SH_0— and S_0—mode waves propagating at 0°, 45°, and 90° to the sheet rolling direction. From theoretical considerations, we expected correlations between $\bar{V}_{SH0}$ and $\bar{r}$, and between $\bar{V}_{S_0}$ and $\bar{r}$. Here, bars indicate an in-plane average; for example, $4\bar{V}_{SH0} = V_{SH0}(0°) + V_{SH0}(90°) + 2V_{SH0}(45°)$ where $V_{SH0}(\alpha)$ is the velocity for the SH_0—mode wave propagating at angle α to rolling direction.

The results of our experiments are shown in Figures 1 and 2.[1-2] In general, there is a (nearly) linear relation, with some scatter about the best-fit line. For example, almost all the data in Figure 1 ($\bar{r}$ vs. $\bar{V}_{SH0}$) lie within a spread

of 0.4 in $\bar{r}$ as measured from the best-fit line. For the data in Figure 2, the spread is about half as much, i.e., there is half the scatter in the plot of $\bar{V}_{S0}$ vs. $\bar{r}$ as in $\bar{V}_{SH0}$ vs. $\bar{r}$. We noted that the data points for the four Japanese sheets (supplied by the same manufacturer) could be fit by a straight line with a spread of about 0.05 in $\bar{r}$.

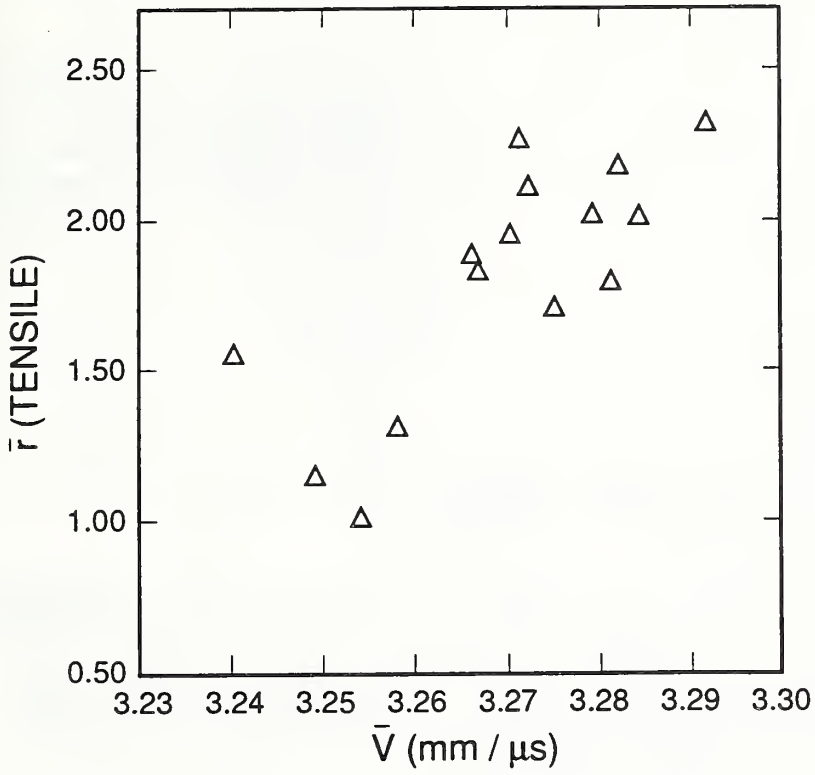

Figure 1. Correlation between mechanical measurements of $\bar{r}$ and ultrasonic measurements of $\bar{V}_{SH0}$.

The fact that the data measured with the S_0-mode had less scatter indicates that this mode may be preferable to use in industrial applications. However, it would be desirable to make measurements on a larger data base of sheet before drawing a firm conclusion on this point.

There may be another practical reason for preferring the S_0-mode over the SH_0-mode. The EMAT design we currently use to generate the latter mode uses an array of permanent magnets of alternating polarity. We find that acoustic Barkhausen noise is generated in our (magnetic) ferritic steel sheet as the SH_0-EMATs are scanned. (Acoustic Barkhausen noise is sound caused by rotation of the magnetic domains as the magnetic field is changed). This may be a serious problem for on-line application on moving sheet.

Another practical consideration is the rapidity of measurement. At present, we use a time-interval-averaging counter, and average 100 arrival times to suppress random electric noise. With our present EMATs, we have a time resolution of better than 1 ns.

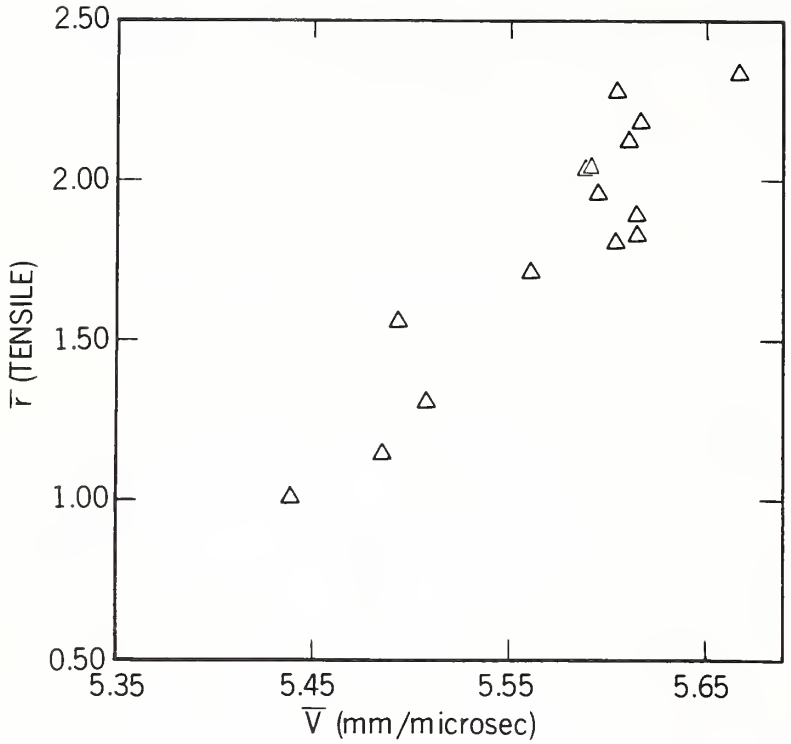

Figure 2. Correlation between mechanical measurements of $\bar{r}$ and ultrasonic measurements of $\bar{V}_{SO}$.

We performed a study to determine if the number of averages could be reduced. We used a high-speed digital oscilloscope to digitize waveforms, and a correlation routine to determine the corresponding arrival times. We found that there was at most 0.3% change in velocity where 10 averages were taken, and about 0.5% change when no averaging was done (single-shot event). This is quite promising for possible on-line application.

A typical scope trace obtained with our system is shown in Figure 3. In some applications, we can obtain signals with peak-to-peak voltages of four volts, with a "noise" background of about 20 mv; thus, our signal/noise ratio can (ideally) be greater than 40 dB.

We have developed a prototype system and demonstrated it to the Advanced Steel Processing and Products Research Center (ASPPRC) at the Colorado School of Mines (Golden, Colorado). The demonstration was attended by researchers from participating ASPPRC institutions, which include major steel and automotive companies.

A collaboration between NIST and Ford Motor Company is now underway to produce an improved version of the above system which will be suitable for an industrial environment. NIST has responsibility for producing EMATs and electronics; Ford will provide mechanical fixturing. The system is intended for off-line use in a quality-assurance laboratory in a Ford stamping mill. When completed, the system will be evaluated jointly by Ford and NIST. Experience gained in this evaluation will be applied to the next phase of the collaboration, which seeks to address on-line implementation in a stamping plant.

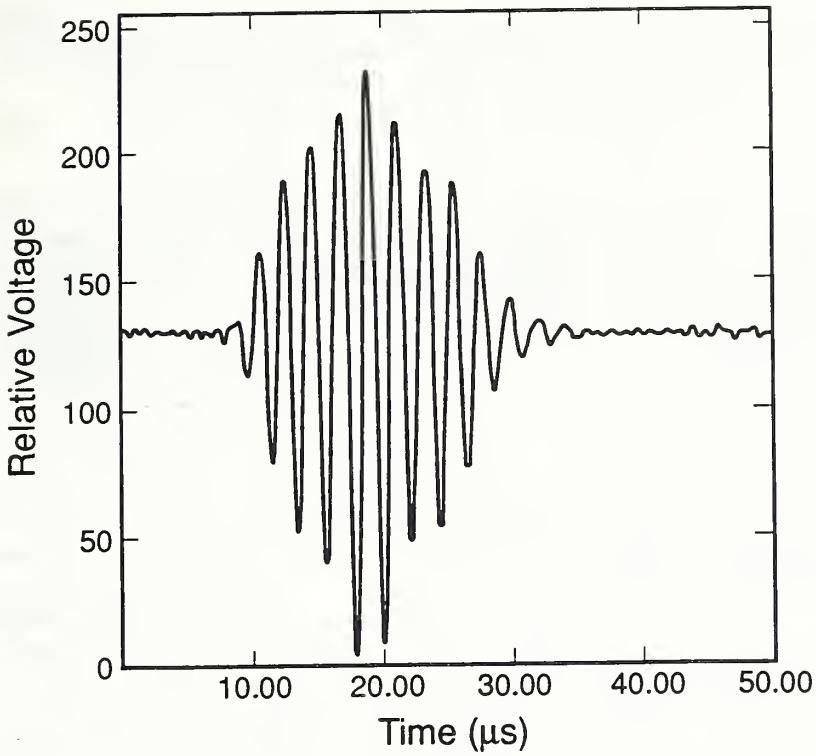

Figure 3. Scope trace showing signal detected by receiving EMAT, and amplified by low-noise high-gain electronics.

References

1. A. V. Clark, R. B. Thompson, G. V. Blessing, D. Matlock, "Ultrasonic Measurement of Formability in Thin Ferritic Steel Sheet," Review of Progress in Quantitative NDE 8A, pp. 1031-1038 (1989).

2. A. V. Clark, R. B. Thompson, R. C. Reno, G. V. Blessing, D. Matlock, "Steel Stamping Technology: Applications and Impact," Paper SP-779 (Soc. Auto. Engrs., 1989).

Ultrasonic Metrology for Surface Finish and Part Thickness

G. V. Blessing and D. G. Eitzen
Automated Production Technology Divison
Center for Manufacturing Engineering

Noncontact sensors for on-line metrology in machining centers are of significant interest for automated manufacturing. In the work reported here, ultrasonic sensor techniques are being developed and evaluated for such applications as the in-process measurement of part surface finish and part thickness.

In previous reports, we presented results demonstrating the capability of ultrasound to monitor the finish of both stationary and rapidly moving part surfaces. Liquid coupling between the ultrasonic transducer and the part surface was achieved either by part immersion or by a guided stream. Both water and machine coolant/lubricants proved to be effective coupling liquids.

Here we first report results obtained on stationary part surfaces using ambient air coupling, of value for those applications where the part is dry for convenience or by necessity. The limiting factors with this approach are air turbulence and thermal gradients between the sensor and the part surface.

To evaluate the sensitivity of airborne ultrasound to surface finish, measurements were made using an area-averaging scattering approach wherein the insonified area is much longer than individual surface features (peak height and spacing).[1] Pulse-echo measurements were made on metal and ceramic surfaces with the incident ultrasound normal to the median surface plane. Representative results are given here using 4.4 MHz ultrasound (75 μm wavelength in air) with a transducer-surface separation of 2 to 3 mm. The insonified surface areas ranged from 1 to 6 mm^2, depending on transducer aperture.

A nickel-plated metal specimen possessing a sinusoidal surface of 100 μm periodicity with three discrete roughness sections was studied. The average roughness values R_a of the three sections were 0.3, 1.0, and 3.0 μm. The resultant ultrasonic echo amplitude values, normalized to unity on the smoothest section, were respectively 1.00, 0.95, and 0.78 $\pm$ 0.01. In another test of airborne ultrasound, a pair of alumina ceramic samples possessing random roughness surface features with respective R_a values of 1.1 and 2.9 μm were studied.[2] The ultrasonic amplitude response from the smoother sample was about 6 dB greater than that from the rougher sample, where the system resolution was about 2 dB. With such a sensor, the manufacturer could seek to eliminate the need for subsequent polishing of its fired ceramic parts by altering process parameters in response to the condition of the monitored surface finish. The results of both tests demonstrate the ability of air-borne ultrasound to resolve surface finishes, whether periodic or random in nature, to better than 1 μm R_a.

An automated ultrasonic system for noncontact one-sided precision thickness measurements has been under development for delivery to the Department of Energy.[3] The goal is to measure nominally 1.5 mm thick parts of rotation in situ to an accuracy of 2.5 μm. The system incorporates a commercial ultrasonic pulser/receiver thickness gauge providing amplitude and transit-time data to a personal computer acting as a controller for sensor motion, and as an analyser/storage/plotting device for the ultrasonic data. It is designed to be integrated with CNC turning center machine software and hardware. Figure 1 illustrates the principal components, with the ultrasonic sensor mounted on a tool turret and positioned to examine the rotating parts (shells) of circular symmetry. The machine motion combined with the sensor angulation provide the capability to orient the ultrasonic beam normal to the part surface for pulse-echo measurements at a nominal frequency of 15 MHz.

A sample output of the ultrasonic thickness data as a function of part rotation angle about the chuck axis is shown in Figure 2. The digitized thickness data is resolved to 1 μm, where each plotted value represents an average of 64 individual transit-time echo measurements. This scan of six seconds, taken on a band of the shell at an azimuthal angle of 70° from the chuck axis, is comprised of 290 such averaged thickness measurements. The center horizontal dotted line indicates the part design thickness, and the pair of horizontal

dashed lines indicate the upper and lower bounds (± 25 μm) of part acceptability.

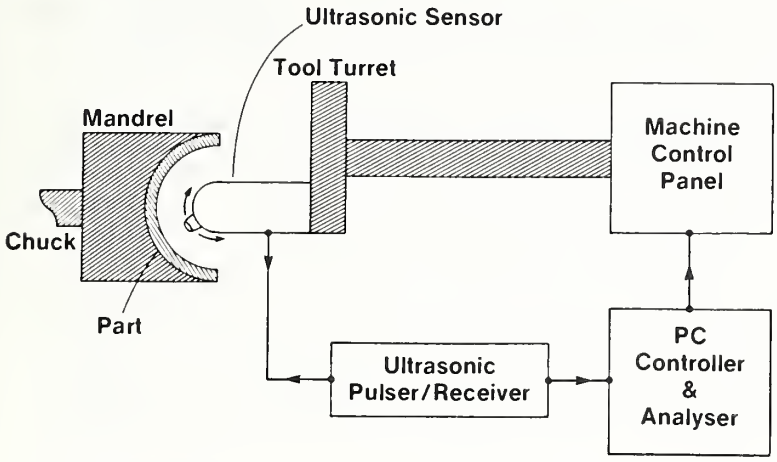

Figure 1. An integrated ultrasonic system for the one-sided noncontact measurement of precision machined parts (shells) in situ on a turning center.

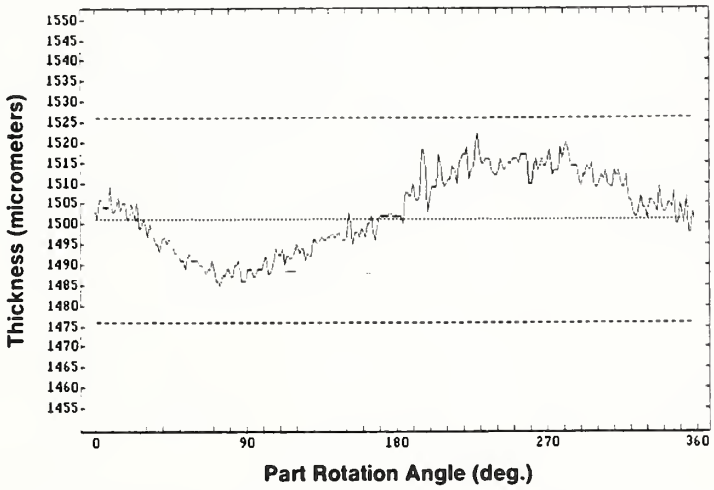

Figure 2. An ultrasonic thickness scan of a circular band on a shell part as a function of the part rotation angle.

Future plans include additional ultrasonic profilometry work on another spatial sinusoid specimen with a wavelength of 100 μm and an R_a of 0.3, 1, and 3 μm. We will also begin work on enhancing the in-situ automated thickness measurement system so that it can determine part surface finish and part form. It may be necessary to develop a hybrid transducer since these various functions will likely be optimized by different frequencies. We will also address a fundamental problem of ultrasonic metrology; a part whose thickness is nonuniform over the beam width, creating phase differences which affect transit time.

References

1. G. V. Blessing and D. G. Eitzen "Ultrasonic Measurements of Surface Roughness and Topography" Proc. of the 3rd International Symposium on Nondestructive Materials Characterization, 3-5 Oct 1988, Saarbrucken, Germany (to be published).

2. Ceramic samples provided by J. Ziegler, McDanel Refractory, Beaver Falls, Pennsylvania.

3. Funded in part by the Dept. of Energy, Rocky Flats, Colorado.

C. NDE FOR COMPOSITES PROCESSING AND INTERFACES

The goal of this activity is to develop generic approaches, sensors, and procedures for quantitative NDE of composites and interfaces. As in the two previous activities, the emphasis is on measurements that can be made during the manufacturing process to sense the properties of the product during critical stages of its formation and to provide the data required to control the process to optimize quality and productivity. Since the knowledge base on composites characterization is far from complete, we expect that a portion of this activity will be concerned with relating important composite characteristics with performance and then developing NDE monitoring methods.

This activity includes research on utilizing fluorescence spectroscopy to monitor the processing of polymer matrix composites, applying ultrasonic techniques to improve the understanding and ability to monitor interfaces, and utilizing photothermal radiometry (thermal wave NDE) to characterize diamond films. A noteworthy accomplishment in this activity:

- A major barrier to the implementation of advanced polymer composite materials in many applications is that the processing lacks the desired reliability. To improve the reliability, NDE measurement techniques need to be developed to improve process monitoring and control. Previous NIST research showed that fluorescence spectroscopy is feasible for polymer process monitoring of non-Newtonian shear viscosity, molecular orientation, velocity, and flow characteristics. These parameters play a key role in determining the properties of composites. During the past year significant achievements have been attained in a number of areas in this effort including the measurement of shear stress, non-Newtonian viscosity, residence time distribution, quality-of-mix of ingredients, and flow instabilities.

Measurement and Control of Polymer Processing Parameters Using Fluorescence Spectroscopy

A. J. Bur, A. Lee, R. E. Lowry, S. C. Roth, and F. W. Wang
Polymers Division
Institute for Materials Science and Engineering

In this program, fluorescence spectroscopy is being employed as a tool to monitor polymer processing parameters that are important for understanding and controlling process behavior. The measurements involve the detection of fluorescence spectra from fluorescent dyes which have been doped into the processed polymer material. The character of the fluorescence, i.e., its intensity, polarization, and wavelength distribution, yields information about the state of the polymer matrix. We have concentrated on developing concepts and methods to measure molecular orientation, shear stress, shear rate, non-Newtonian viscosity, velocity, flow instabilities, quality-of-mix of ingredients, residence time distribution, and intersegmental mixing. Work on each of these measurement problems is ongoing and in various stages of development. During the past year significant achievements have been attained in the measurement of shear stress, non-Newtonian viscosity, residence time distribution, quality-of-mix of ingredients, and flow instabilities. In addition, we have established a model

for the behavior of the velocity/shear rate probe and we have selected a polarity sensitive fluorescent dye which can be used to monitor intersegmental mixing.

During the past year, we achieved the first application of fluorescence monitoring to the processing environment by installing an optical fiber probe at the exit die of a twin screw extruder. The experimental set up, which was located at the Naval Surface Warfare Center, is diagrammed in Figure 1. In this process, a polymer melt (polybutadiene) is combined with solid particulate ($CaCO_3$) at 65% volume concentration, mixed by the action of the twin screws and extruded through the exit die in the form of rod approximately 1 cm in diameter. The objective of the fluorescence measurements was to observe residence time distribution. A fluorescent dye, coumarin 30, is "instantaneously" injected into the dye port which was 62 cm upstream from the exit die. The dispersion of the dye in the mixture is depicted in the fluorescence intensity vs time plot of Figure 2. We see that the delta function distribution at the time of dye injection is transformed into a dispersion which extends over several minutes, indicating the extent of spatial mixing and transport of dye in the extruder.

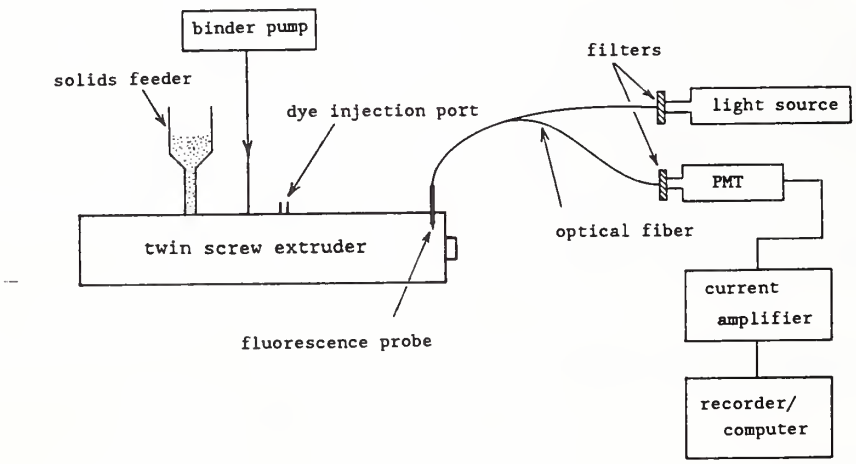

Figure 1. The experimental arrangement for observing residence time distribution, flow instabilities, and quality-of-mix of twin screw extruder processing is shown. The separation between the optical fiber probe and the dye injection port was 62 cm.

In Figure 3, we plot similar data for $CaCO_3$ concentration of 70% by volume. By contrast with the data of Figure 2, flow instabilities occurred in this case because of the formation of particulate mats which stopped the flow of material until a pressure buildup was large enough to break the mat. This is seen in the fluorescence vs time data as steps or regions of constant fluorescence intensity which occurred when flow was stopped. This is followed by an immediate decrease or increase in the fluorescence intensity as pressure forced flow proceeds until the next cycle of mat formation occurs. In future experiments, we will correlate these data with pressure and torque observations and carry out measurements of quality-of-mix of ingredients by observing the fluctuations in fluorescence intensity as a function of time.

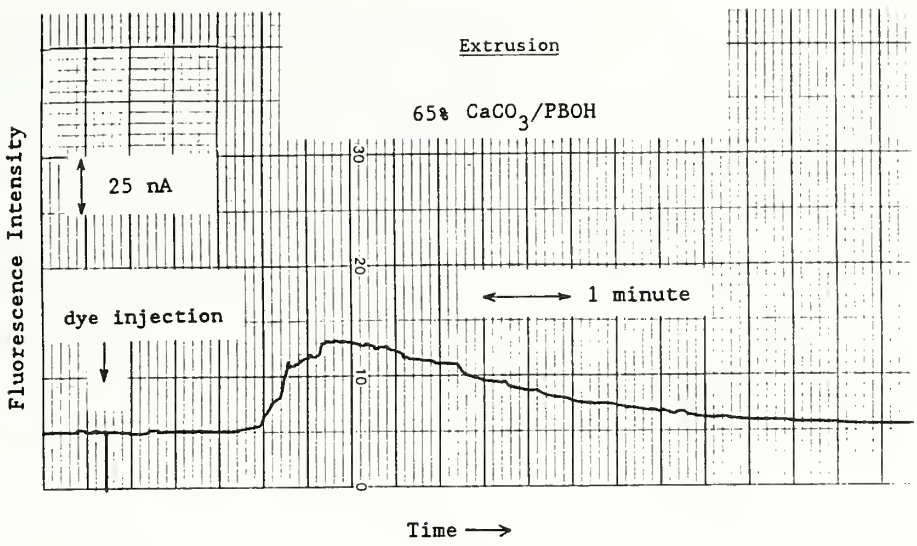

Figure 2. Fluorescence intensity vs time is shown for the twin screw extrusion of polybutadiene mixed with $CaCO_3$ at 65% by volume. The curve is a residence time distribution for the coumarin dye that was injected into the flow stream at the dye injection port.

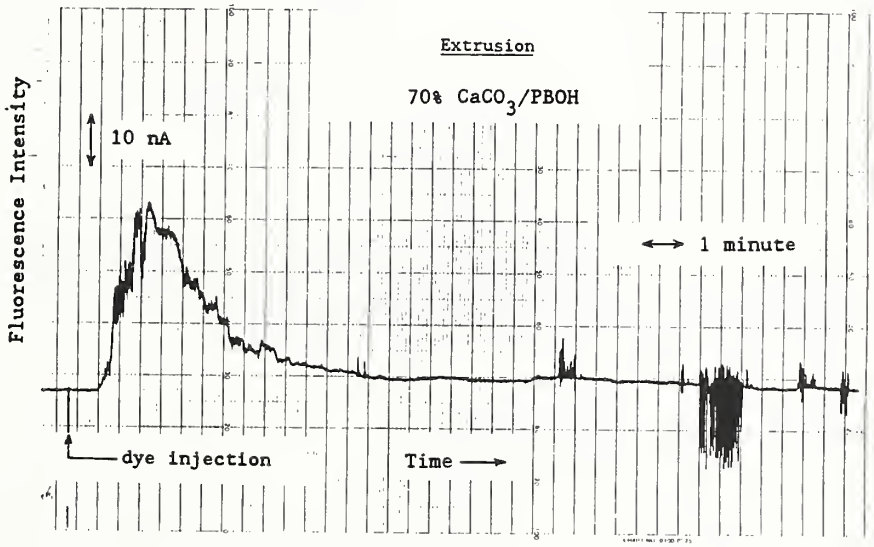

Figure 3. Fluorescence intensity vs time is shown for the twin screw extrusion of polybutadiene mixed with $CaCO_3$ at 70% by volume. The basic shape of the curve is a residence time distribution that is altered by the effect of flow instabilities.

The measurement of fluorescence anisotropy can be used to determine shear stress, molecular orientation, and non-Newtonian viscosity. The measurement involves the use of polarized light to determine the orientation of the fluorescent dye. Laboratory confirmation of this measurement concept was achieved by using a polymeric fluorescent dye, polybutadiene tagged with anthracene,

which was prepared in our laboratory. This dye was doped into a cetane solution of polyisobutylene (PIB) at 0.1% concentration by weight and its fluorescence anisotropy was monitored as a function of shear rate using a cone and plate rheometer. The results are shown in Figure 4 where we have plotted shear stress, shear viscosity, and anisotropy versus shear rate. We note that the PIB solution is non-Newtonian in this range of shear rates which means that, as viscosity decreases with increasing shear rate, molecular orientation in the direction of the flow field occurs. This is reflected in the fluorescence anisotropy, which increases with shear rate and indicates that the fluorescent dye has been incorporated into the PIB matrix and follows the matrix orientation. We plan to apply this measurement concept by fabricating an optical fiber probe for on-line measurement of fluorescence anisotropy from which shear stress and non-Newtonian viscosity can be deduced.

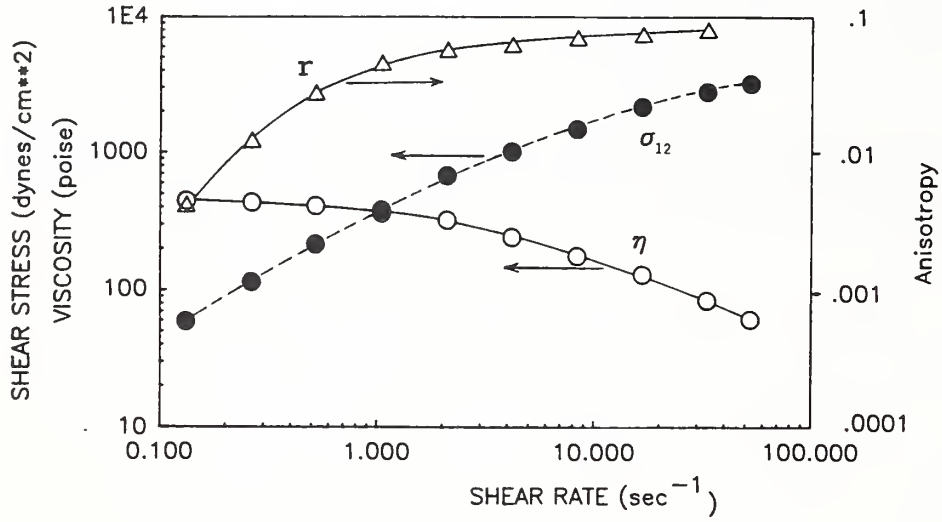

Figure 4. Shear stress (σ_{12}), fluorescence anisotropy (r), and non-Newtonian viscosity (η) are plotted against shear rate for a cetane solution of polyisobutylene doped with antracene tagged polybutadiene.

Nondestructive Evaluation of Diamond Films

H. Frederikse*, A. Feldman and X.T. Ying**
Ceramics Division
Institute for Materials Science and Engineering

*Consultant to NIST
**Guest Scientist from Fudan University, Shanghai, Peoples Republic of China

The objective of this project is to evaluate the quality of ceramic films used as thermal barriers and as heat sinks, with particular emphasis on synthesized diamond films, by means of thermal wave methodologies. Chemical vapor deposited (CVD) diamond films hold considerable promise for technologically important applications due to the unique properties of diamond: greatest hardness of any material, highest room temperature thermal conductivity of any material,

high electrical resistivity, chemical stability under extensive conditions, and optical transparency over wide wavelength ranges. The thermal properties are important for determining the performance of diamond in applications requiring the dissipation of heat. In addition, the thermal conductivity provides an important measure of diamond quality; the higher the quality of the diamond film, the larger the value of the thermal conductivity.

During the past year our accomplishments have included measuring the thermal properties of CVD diamond films. We have used the technique of photothermal radiometry (PTR) to obtain the thermal diffusivity, α, and thermal conductivity, κ.

The conventional PTR method, which is the technique currently implemented, (discussed in ONDE Technical Activities Reports for 1987 and 1988) is suitable for thick films of CVD diamond. An unsupported CVD diamond specimen, 0.25 mm in thickness, was made available to us by T. Anthony of the General Electric R&D Center. Measurements on this sample were performed at five temperatures between 300 and 700 K; the relative phase, $\Delta\phi$, of the modulated temperature was recorded as a function of the modulation frequency. Fitting $\Delta\phi$ vs $\sqrt{f}$ to the theoretical expression for one-dimensional heat propagation normal to the surface yielded values for α over the indicated temperature range. Using handbook data for the specific heat, C, and density, ρ, we calculated κ. Figure 1 shows the temperature dependence of κ for the CVD diamond specimen and for single crystal diamond.[1] At room temperature κ of the CVD diamond is considerably smaller than κ of the single crystal. This can be attributed to the small size of the crystallites in the diamond film. However, with increasing temperature, κ of the CVD diamond increases, reaching the value for the single crystal diamond at about 700K.

Thin diamond films pose a problem for the conventional PTR technique. This is because the technique relies on the use of thermal waves with thermal diffusion lengths comparable in size to the film thickness. With film thicknesses in the range 5-10 μm, modulation frequencies $\geq$ 1 MHz are required; however, commercial lock-in amplifiers, which are used in these experiments, will operate only to several hundred KHz. Therefore, we have used a different approach for thin CVD diamond films. In this approach, we employ heat that flows parallel to the surface of the film. The diamond films used are deposited on strips of mullite, an alumina-silica compound. Mullite was chosen because of its low thermal conductivity; this minimizes heat transfer from the diamond film, and because of its thermal expansion that matches the thermal expansion of diamond which minimizes stress-induced cracking in the diamond (previously observed when fused silica substrates were used.) The film dimensions were approximately 1 mm x 20 mm x 5 μm. A modulated laser beam heated a blackened spot on one end of the film and the temperature of another blackened spot on the film, a distance 1-2 mm from the heated end of the sample, was measured by means of an infrared detector. In this geometry the heat loss to the substrate is small but not negligible and therefore a loss term should be included in the heat flow equation. We assume we can use the one dimensional heat diffusion equation, modified to include loss, given by[2]

$$\frac{\partial^2 T}{\partial x^2} = \frac{1}{\alpha}\frac{\partial T}{\partial t} + hT \qquad (1)$$

where h is the coefficient for heat loss in Newton's law of cooling. The modulated temperature distribution T(x) at frequency f will decay exponentially with distance x, and the log decrement of T(x) will have the form

$$\ln\left(\frac{T(x)}{T(0)}\right) = x\left(\frac{(h^2+\omega^2)^{1/2}+h}{2\alpha}\right)^{1/2} \qquad (2)$$

where $\omega = 2\pi f$.

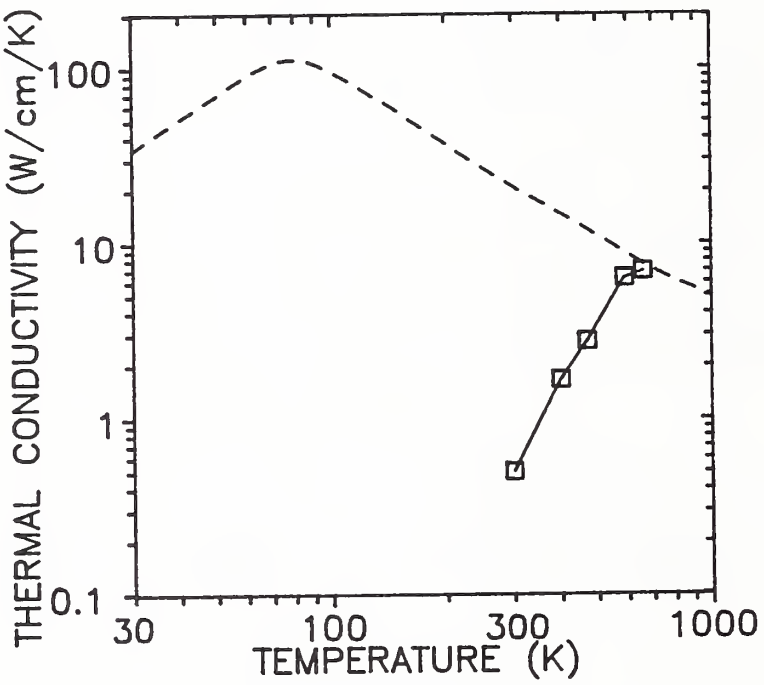

Figure 1. The temperature dependence of the thermal conductivity of a CVD diamond specimen (squares) compared with the thermal conductivity of bulk diamond (dashes). The values for bulk diamond above 300K are extrapolated.

By measuring the decrement at two frequencies f_1 and f_2 the parameters h and α can be calculated. At high frequencies (ω>>h) the slope of the log decrement vs $\sqrt{f}$ becomes $\sqrt{(\pi/\alpha)}$. Due to the rapid attenuation of the signal with x, the measurements could not be extended beyond f = 200 Hz. The results obtained are presented in Table I. We have observed that the specimen produced with 0.25% methane/H_2 ratio has a lower thermal diffusivity than the specimen with 0.5% methane/H_2 ratio. This is contrary to the results of Ono et al.[3] and may be explainable by variations in other deposition conditions.

TABLE I. Thermal Diffusivity α and Thermal Conductivity κ of Thin Diamond Films

Sample #	Percent Methane	α cm^2/s	κ W/cm.deg
147	0.25	0.29-0.38	0.52-0.68
155*	0.50	0.92-1.14	1.66-2.05

*Sample #155 is a free-standing film resulting from etching away the silicon substrate.

Efforts are underway to improve the geometry and the analysis of the transverse photothermal radiometry method as applied to thin films with high thermal conductivities on dielectric substrates.

References

1. R. Berman, E. L. Foster and J. M. Ziman, Proc. Roy. Soc. A237, 344 (1956).

2. J. E. Parrott and A. D. Stuckes, Thermal Conductivity of Solids, Pion Limited, p. 24 (London 1975).

3. A. Ono, T. Baba, H. Funamoto, and A. Nishikawa, Jap. J. Appl. Phys. 25, L808 (1986).

Transient Elastic Waves in Laminates

N. Hsu, S. Ren*, and D. Eitzen
Automated Production Technology Division
Center for Manufacturing Engineering

*On leave from Institute of Acoustics, Chinese Academy of Sciences, Beijin, China

Pulsed ultrasonic testing techniques have been proposed for a greater role in the evaluation and quality control of composite materials. The understanding of the generation of ultrasound, its interaction with interfaces in the material, its detection and interpretation constitutes an important part of the development of the technology. Our approach has been a multi-faceted one. The four domains of exact theory, numerical simulation, controlled laboratory experiment, and field applications are designed to have overlapping regions so that assumptions can be checked and solutions have immediate practical usages. The current project is to develop the ability to model, exactly, the generation, propagation, reflection and refraction, and detection of point source ultrasonic waves in layered media. Specifically, it was proposed to derive and design algorithms to compute the exact dynamic Green's function of a layer

of uniform thickness on a half-space for various material properties and various interface (bonding) conditions.

In the past we developed and made available to the public a Fortran code to compute the dynamic Green's function of an infinite plate. The computation has many proven practical applications, among them: calibration and design of transducers, design and verifaction of laser generation and detection of ultrasound, development of novel testing techniques, and acoustic emission source characterization. It has been utilized by federal labs, universities and industry. The code also serves as a check of the present program being developed.

During the current year we successfully completed the following tasks:

a. Derivation of the formulas for a multi-layer structure based upon J. Willis's method.

b. Designed algorithms and wrote Fortran code for a single layer on a half-space with three different bonding conditions between the layer and the substrate. This consists of many modular subroutines to compute: time of arrival of all successive rays, a summation scheme for multiple ray paths with the same arrival time, reflection and refraction coefficient matrices and a contour integral path which avoids singularities.

c. The program is being developed on an inexpensive personal computer. It can easily be transferred to other types of computers (e.g., Compaq) for improved speed.

In Figure 1 are sample results of the computation. These curves are the computed vertical displacement as a function of time due to a point contact source transducer; its contact force as a function of time is shown as the inset.
The resulting displacement for three cases corresponding to three interface conditions shown: (a) no bonding - free boundary, (b) welded bond - both stress and displacement are continuous across the boundary, and (c) liquid bond - normal stress continuous at the boundary. The test configuration and the material properties used in the computation are given in the caption. The result shows that by monitoring the expected arrivals of head waves and by examining details of the reflected shear wave one can deduce the conditions of the bond.

A controlled experiment of a plexiglass plate on an aluminum block is planned and will be carried out in the next year. Documentation of the computer program is also planned if time permits. In addition, a thorough examination of the generation and evolution of the interface wave for various dissimilar layer and substrate materials is being carried out. The close examination may bring new ideas for testing adhesive bonding and composite strength using tailored interface transient waves.

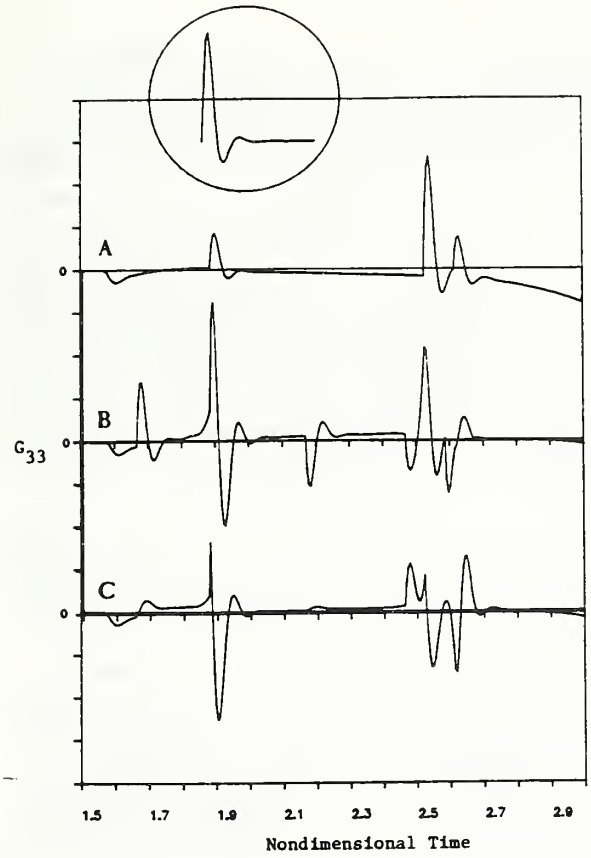

Figure 1. The curves in the figure are the theoretically computed Green's functions G_{33} for the case of a plexiglass layer overlay on a glass substrate when both the source and the detector are located on the top surface of the layer and the distance between them is three times the thickness of the layer. The input force is an exponential sine function shown as an inset in the figure. The longitudinal wave speed and shear wave speed of the plexiglass and the glass are respectively 2730, 1430, and 5830, 3490, the units are (m/s); the densities are respectively 1180 and 2500, the units are (Kg/m^3). Three curves correspond to the different boundary conditions of the interface while the top surface of the layer is traction free.

a. Traction free boundary condition.
b. Welded boundary condition.
c. Liquid coupled boundary condition.

Intelligent Processing of Solder Joint Connections for Printed Wiring Assemblies

H. T. Yolken and L. Mordfin
Office of Nondestructive Evaluation
Institute for Materials Science and Engineering

The Office of Nondestructive Evaluation has received a multi-year contract from the Harry Diamond Laboratories to carry out a major portion of a new DoD program to develop an intelligent processing system for solder joint connections on printed circuit boards. In military applications these must function reliably under conditions that are frequently adverse, e.g., temperature extremes, mechanical shock and vibration, and corrosive environments. The goal of the DoD program is an automated or intelligent processing system for solder joints that will minimize rejects and boost the long-term reliability of electronic hardware. NIST will develop a materials property database and evaluate nondestructive evaluation instruments for the system.

An intelligent processing system employs non-intrusive sensors to monitor characteristics of a material while it is being processed. The sensor signals feed into a computer that controls the process parameters in such a way as to avoid the manufacture of sub-quality products. Control decisions are made on the basis of an expert system, a process model, and a database.

The system under development, as it is presently envisioned, uses a laser soldering facility that scans the boards according to a pre-programed raster pattern. A laser scattering technique characterizes the shape of each solder bead as it is made, and in-process nondestructive evaluations assess the quality of each connection.

ONDE has assembled a cooperative project involving several NIST organizations to address some important segments of the DoD program. The largest segment is the development of a database on the mechanical, electrical, and thermal properties of solder joint materials. This segment is being carried out in the Metallurgy Division in collaboration with the Army's Materials Technology Laboratory. The work involves: (1) the characterization of the metallurgical phases present in electronic solder connections, (2) the synthesis in bulk of these alloys and intermetallic compounds, and (3) the measurement of their properties.

Computer scientists in the Center for Manufacturing Engineering are developing an algorithm to generate a finite element mesh for each solder bead so that a fracture mechanics analysis can be computed immediately if a flaw is found in the joint by the nondestructive evaluation sensors.

One of these sensors is an x-ray laminography instrument for detecting internal flaws in solder joints, and another is an infrared reflectometry instrument which assesses the quality of both the bead surface and its connection to the substrate. Engineers and scientists in the Fracture and Deformation Division and in the Center for Manufacturing Engineering are evaluating these two commercial NDE instruments. They will recommend modifications, if needed, and will prepare operating manuals for use by factory personnel.

D. NDE STANDARDS AND METHODS

The objective of the Standards and Methods activity in the NDE Program is to provide the scientific understanding of NDE measurement methods and to develop, maintain, and disseminate effective standards for NDE measurements that are traceable to national standards.

Six project reports from the NDE Standards and Methods activity are presented this year dealing with ultrasonics and acoustic emission, eddy currents, magnetic methods (primarily Barkhausen), real-time radiology, thermography, and the capacitive array sensor. All six of the reports document significant progress. It is fair to say that the NDE Standards and Methods activity is the cornerstone of the entire NDE Program, as it continues to serve as the basis for intensive standardization and consultation services provided to the nation's NDE community.

The Program's temporary halt of research on leak testing methods and standards due to staffing problems, which was reported last year, was not intended to imply any curtailment in NIST's measurement services for leak testing. On the contrary, the Special Test Service for helium leaks completed ten tests this year, most of them on leaks near the lower end of our calibration range, 10^{-11} mol/s. Research next year will begin to address demands for extension of our capabilities to even smaller leakage rates and to gases other than helium, and a workshop on the helium leak calibration service will be conducted at the 1990 Measurement Science Conference.

A few brief illustrations of this year's accomplishments in the NDE Standards and Methods activity follow.

- NIST's system for primary calibration of acoustic emission (AE) transducers, which was adopted by ASTM in 1986 and is used in several other countries as well, was formally submitted to the International Organization for Standardization. A promising approach to a secondary calibration scheme for AE transducers, involving a relatively portable transfer standard, was developed this year. Both calibration schemes utilize the NIST conical transducer, for which Tom Proctor of the Center for Manufacturing Engineering was granted an IR-100 award in 1981. A new implementation of Proctor's approach, a tangential transducer that measures dynamic motions parallel to a surface, was awarded a patent late in 1988.

- ONDE's long-term contract from the Army Materials Technology Laboratory to develop new and improved military standards for NDE was again fruitful this year. MIL-STD-1949A, an updated version of the 1985 standard on magnetic particle inspection, was issued 15 May 1989 on the basis of Lydon Swartzendruber's work in the Metallurgy Division. (Swartzendruber was also the author of the original version.) The new document is the world's most advanced standard on magnetic particle testing. A new military standard on radioscopic inspection was drafted by Tom Siewert of the Fracture and Deformation Division in collaboration with GE scientists. This document is currently under review in the industrial community.

- A new "Test Method for Minimum Detectable Temperature Difference," which was developed in the NDE Program, was issued by ASTM this year as Standard E 1311. This is the second of three test methods that are being developed by NIST in order to characterize the critical performance parameters of thermographic NDE instruments. The third test method, dealing with measurements of the noise-equivalent temperature difference, is expected to be ready for critical review in a few months.

- Tom Capobianco of the Center for Electronics and Electrical Engineering developed a method for producing tight discontinuities, in metal surfaces, that provide eddy current signals that closely simulate those from hairline fatigue cracks. The artificial cracks appear to offer significant advantages over real fatigue cracks or EDM notches as artifact standards, for calibrating eddy current NDE systems, because they are highly reproducible and can be made to preselected dimensions. Structural aluminum alloy blocks containing the artificial cracks have been offered for sale by the Office of Standard Reference Materials as Research Material 8458.

Ultrasonics and Acoustic Emission

D. G. Eitzen and the Ultrasonic Standards Group
Automated Production Technology Division
Center for Manufacturing Engineering

The objective of this project is to develop and disseminate artifact and documentary standards, develop and maintain measurement and calibration services, and develop new or improved methods for acoustic emission (AE) and ultrasonic NDE techniques. The writing of documentary standards is preceded by extensive and careful measurements and analysis to form an adequate technical base and, frequently, by the design and piloting of round robins. The standards are typically guided through ASTM and then promoted as international standards.

NIST's calibration services for acoustic NDE methods are essential to the NDE community and are world-class. Significant effort is needed to maintain these services and, in some cases, to expand the capabilities, e.g., AE sensor calibration for composite structures in the chemical and aeronautics industries.

Our transducer development work is motivated by the need for devices to transfer calibrations to sensor users/suppliers, and by the need for precision dynamic motion measurement for new or advanced acoustic techniques. The development of new ultrasonic and AE techniques also relies heavily on theoretical analysis to gain a better understanding and new insight into the physics of the sound-structure interactions.

Our documentary standards activities were again extensive and fruitful in 1989. Under the auspices of ASTM Committee E 28 we are working on a draft standard on ultrasonic measurement of bolt tension and have drafted a recommended practice for construction and use of a stepped reference block to determine the accuracy of speed of sound measurements. A round robin has been piloted on using an alternative instrument to compare ASTM E 127 type

reference blocks. The results are, so far, encouraging and will lead to a major revision of the E 127 standard practice. A working draft on primary AE sensor calibration based on the NIST technology has been distributed within ISO and, after minor modification, will be balloted for elevation to Draft Proposal status.

Secondary Calibration of AE Transducers

The design of a practical and reasonably accurate transfer (secondary) calibration system for acoustic emission transducers evolved in the past year. This involved the use of a 20-cm-thick block which replaced the 3.3-cm-thick plate that was found to be unsuitable last year. The calibration scheme used as a test of the suitability of the transfer block is very similar to that of the primary calibration. The test scheme uses a capillary-break source located near the center of one of the large faces of the block and has the transducer under test and the reference transducer each located 10 cm from the source, but in opposite directions. The capillary break produces, on the surface of the block, a pulse which, because of geometric symmetry, excites both transducers equally. Transient waveforms from both transducers are captured, analyzed for frequency content, and compared. A correction based on the primary calibration of the reference transducer is applied in calculating the final calibration data for the transducer under test.

This transducer calibration scheme had been tested early this year using a steel plate 90 cm square by 3.3 cm thick. The size and shape had been chosen to obtain a large area, allowing a long working time, and an overall weight affording some portability compared to that of the primary reference block. Experimental results later showed that in trading off area, thickness, and overall bulk, the thickness of the plate had been reduced excessively. Trial calibrations utilizing both capillary-break and tone-burst schemes were performed on this plate, and the calibration results showed no agreement with the primary calibration results for the same test transducers. The discrepancies have been attributed to excessive variations in the surface displacement of the plate underneath the transducer being calibrated. Such variations would (in hindsight) be expected to be significant when the diameter of the transducer is comparable to the thickness of the plate. We intend to investigate the problem of disparate motion within the aperture of a circular transducer on a plate by a theoretical analysis which uses an integration technique applied to the Green's function for the elastic plate.

The new transfer calibration system utilizes a steel transfer block 40 cm square and 20 cm thick. This block, mounted on casters, is reasonably portable. In the interests of good ultrasonic coupling, it is necessary that at least one of the block's 40 cm square faces have a high quality finish. Blanchard grinding was used to finish both square faces of our block. Since this block is approximately half the size, in linear dimensions, of the primary calibration block, the working time between arrival of the calibration signal and the arrival of its first reflection from the walls of the block is only about half of that for the primary block. For transducers that have a long ringing time when shock excited, the accuracy of the small-block calibration is less. This effect might be expected to be prominent mainly at the low end (100 kHz) of the frequency range.

To evaluate the transfer calibration method, six transducers were calibrated using both the primary calibration system and the proposed transfer calibration system. Three models of transducer were represented among the six. The best results were obtained for an NIST conical transducer, for which agreement was within ±1 dB for almost all points over the calibration frequency range of 100 kHz to 1 MHz (Figure 1). One model of commercial ultrasonic/AE transducer produced results that were in agreement within ±1 dB for almost all frequencies up to 750 kHz, above which the disagreement became as large as 11 dB. For another model of commercial AE transducer the agreement was within ±2 dB almost everywhere, which is approximately as well as the primary calibration can be repeated for this model.

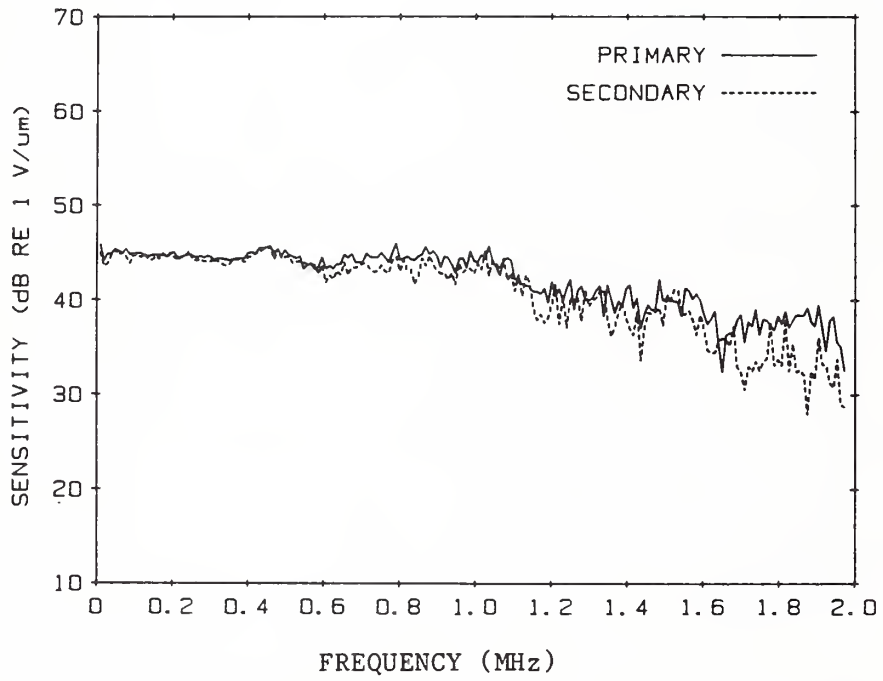

Figure 1. Comparison of a primary and a transfer (secondary) calibration performed on an NIST standard reference conical transducer (SRM 1856).

Elastic Impact Experiments

The study of the impact of elastic spheres on an elastic plate has triple significance: firstly, the impact source has possible application in other AE experiments and in nondestructive testing; secondly, the development of the technique whereby the signature of a source event may be characterized is important; and thirdly, the experimental validation of the theoretical Green's function and deconvolution techniques used in this experiment is essential to all AE studies. In the experiments, steel balls of various sizes were dropped onto a glass plate from a height of 3 cm. A calibrated NIST conical transducer, located on the plate opposite the point of impact, was used to record the displacement of the plate at the transducer location. Deconvolution by the plate Green's function and the transducer response yielded the force-versus-time waveform of the source.

Calibration of the conical transducer had been performed on the same glass plate that was subsequently used in the experiment, because transducer calibration is dependent on the elastic properties of the driving medium. To calibrate the transducer, glass capillaries were broken at a point on one flat surface of the plate, with the transducer located on the other surface and opposite the source. Waveforms from eight calibration events were captured and, for each, the force of the capillary break was measured. It was assumed that the glass-break event applied a Heaviside force to a point on the surface of the glass plate. The captured output waveform from the NIST conical transducer should, therefore, be $F_0 \times H(t) * G(t) * T(t)$, where F_0 is the magnitude of the Heaviside force, H(t) is the Heaviside function, G(t) is the Green's function for the plate, and T(t) is the impulse response of the transducer. Since F_0 is known from the force measurement and G(t) is known from theory, the impulse response of the transducer can be extracted from the captured waveform data by division, differentiation, and convolution operations. The impulse response of the transducer so obtained is inverted with respect to the convolution operation for its subsequent use in the ball-drop part of the experiment. Balls were dropped onto the same spot of the glass plate where the capillary breaks took place, and waveforms from the NIST conical transducer were captured as before. Now, the captured waveform should be $B(t) * G(t) * T(t)$, where B(t) is the force waveform produced by the ball's impact on the plate. B(t) is extracted from the captured data by convolution operations using the known G(t) and T(t). The computational procedures are charted in Figure 2.

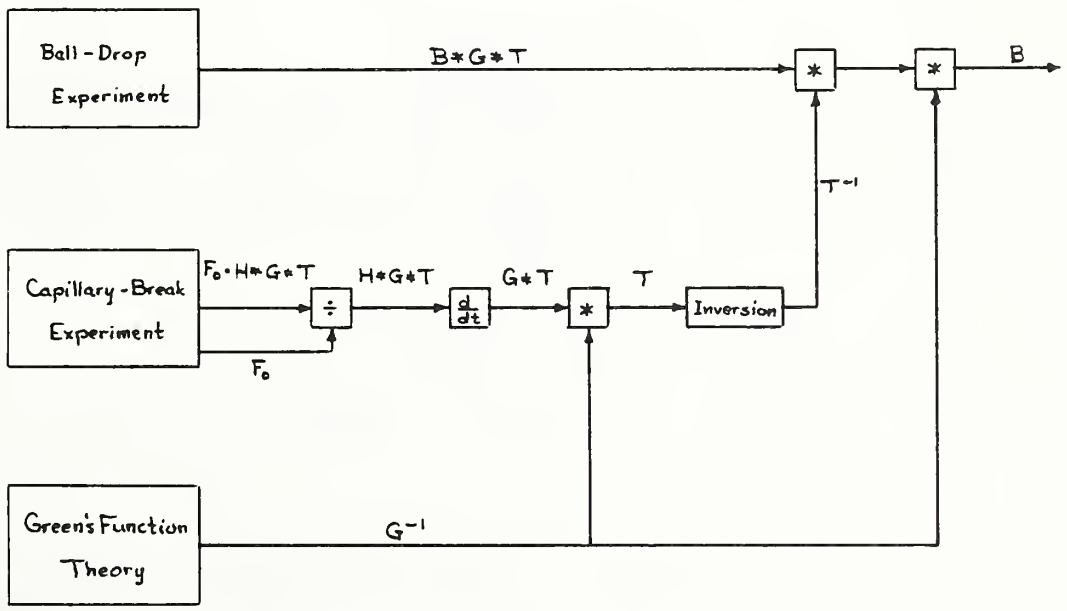

Figure 2. Calculation diagram for the elastic impact experiment. The "*" indicates convolution and the "-1" superscript indicates the convolutional inverse. F_0 is the measured value of the force of the capillary break. The other letters all indicate functions of time: B is the ball-drop force, H is the Heaviside function, G is the Green's function for the plate, and T is the transducer impulse response.

We devised a numerical integration procedure based on Hertz's theory to calculate the theoretical time waveform for an elastic sphere colliding with an elastic plate. The theoretical time waveform so obtained compares very favorably with the results of the dropping ball experiments. Figure 3 shows the theoretical time waveform and the experimental waveform obtained from the single dropping of a 9.52 mm ball. The theoretical data for the curve of Figure 3 was multiplied by 0.9713 for reasons discussed below.

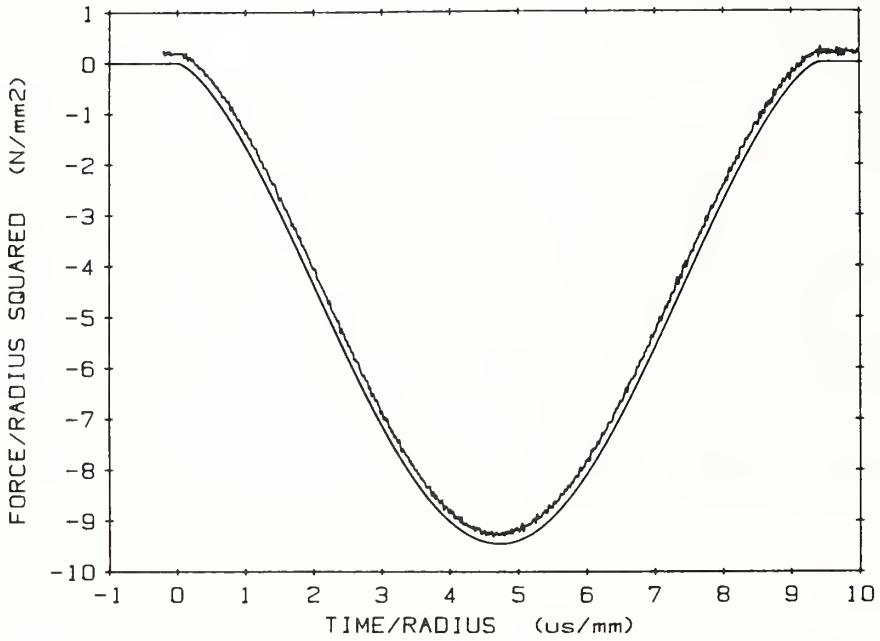

Figure 3. Elastic sphere collision experiment: The lower curve is the force signature of an elastic ball colliding with an elastic plate as calculated from Hertz's theory. The upper curve is the output from an NIST conical transducer after deconvolution by the Green's function for the plate and the impulse response of the transducer. The values for the theoretical curve have been multiplied by 0.9713, and the experimental curve has been elevated by 0.2.

In the elastic collision experiment there were ten balls, each of a different size. The number of dropping events for each size was between seven and ten. For each ball, the average peak force excursion relative to the theoretically predicted force excursion is shown in Table I. The relative peak force excursion averaged for all events is 0.9505, i.e., the impulses obtained in the experiments were small by approximately 5%. The fact that the experimentally obtained impulses were small is not surprising. It is expected that there would be losses owing to sound radiated into the plate and into the air, and possibly other losses owing to air resistance and imperfect elasticity, which are not accounted for in the theory. We calculate that for an impulse that is 0.95 times the theoretical value, there would correspond a coefficient of restitution (ratio of emerging to impinging speed of the ball) of 0.90. Typically, coefficients of restitution do not exceed 95% in such experiments.

The favorable results obtained in the elastic collision experiment validate the use of the technique as a tool to obtain the signature of any impulsive type of source applied to the surface of a plate.

Ultrasonic Power Measurements

The radiation force balance (RFB) serves as the primary NIST means of measuring ultrasonic power. A major modification of the RFB was completed this year. The electromagnetic driver which generates the nulling force to balance the ultrasonic radiation force was extensively modified, a laser interferometer was added for accurate and convenient measurement of the electromagnet's B1 product, and the electronics of the RFB were completely redesigned and built. This has reduced the uncertainty of the device by a factor of three and admits the use of pulsed rf drive for the transducer under test (previously only modulated CW drive was possible). This will greatly expand the utility of the RFB for transducer output measurement.

Tangential Transducer

The tangential transducer, reported in 1986, was awarded a patent[1] and a detailed article describing it was been published.[2] Construction of replicates has begun in order to assure manufacturability and efficient technology transfer. Data are also being collected to verify the agreement between measured waveforms and theory and to demonstrate the added AE information available.

TABLE I. Summary of Ball-Drop Data

Ball Diameter	Peak Force (Experiment/Theory)	Number of Events
9.520 mm	0.9713	7
7.935	0.9587	9
7.134	0.9614	9
6.347	0.9469	8
5.555	0.9557	9
4.760	0.9535	9
3.967	0.9552	9
3.170	0.9254	9
2.377	0.9531	10
1.582	0.9280	9
Average	0.9505	Total 88

References

1. T. M. Proctor, "Transducer for Measuring Transient Tangential Motion," U.S. Patent No. 4,782,701, Nov. 8, 1988.

2. T. M. Proctor, Jr. "A High Fidelity Piezoelectric Tangential Displacement Transducer for Acoustic Emission," J. Acoustic Emission 7, No. 7, 41-48 (1988).

Real-Time X-Ray Radioscopy

T. A. Siewert and D. W. Fitting
Fracture and Deformation Division
Institute for Materials Science and Engineering

The technique of real-time radioscopy uses x-rays, like film-based radiography, but replaces the film with an imaging system. This substantially decreases the fixed costs of inspection and permits continuous (real-time) inspection. Yet, use of this technique has been limited by the absence of standards that can adequately assess the image quality. This program is eliminating the barriers to greater usage of this technique by quantifying the standards needs, developing new standards, evaluating the utility of existing designs for image quality indicators, and developing improved image quality indicators.

An initial task in the program was to assess the needs for standards in real-time radioscopy. We described this program at ASNT, ASTM, and DOD meetings[1-3] and distributed a survey form to interested participants. The 21 respondents included military and civilian system users, equipment producers, and independent consultants. The responses were integrated into a summary report for an ASME conference[4] and a detailed report published this year in Materials Evaluation.[5] This detailed report provides the data to guide the design of new image quality indicators.

Existing image quality indicators were developed for film-based applications. As such they were not designed to measure all the variables that might influence the quality of a real-time image. Specifically, existing image quality indicators cannot measure the effect on the image of specimen translation or rotation. To remedy this situation, we considered the features that should be included in an image quality indicator and proposed a new design, a low-density sphere with a thin high-density coating. A number of these spheres have been constructed and evaluated on three real-time inspection systems. The evaluations confirm several advantages of the spheres, specifically the ease of locating its position in the field of view, the measurement of geometrical magnification in microfocus systems, and the invariance of this information with rotation. A report of this evaluation is being prepared for ASTM Committee E07.01.

These spheres were also evaluated from a more theoretical point of view. High-resolution radiographs were compared with energy absorption profiles obtained by Monte Carlo modeling. The model incorporated photoelectric and Compton attenuation processes to model radiation transport through a two-dimensional representation of the sphere cross section. The model used tabulated photon interaction data for materials in a 12.5-mm-diameter lucite sphere with a 0.03-mm-thick Cu coating. The spheres were radiographed at several kVp levels using a fine-grained industrial film.

The radiographic image of the sphere was quantitatively assessed with a microscope and associated image processing system. This system produced an image intensity distribution across the sphere cross section with a resolution (finer than 0.02 mm) limited by the grain size of the radiographic film. The

quantitative evaluation of this study is being presented at the 1989 Quantitative Nondestructive Evaluation Meeting.[6]

Development of a radiation transfer standard for real-time radioscopy is proceeding in cooperation with ASTM. The ASTM task force in which this effort fits (E07.01.05) is struggling with the general topic of radioscopic system qualification. We have recommended a survey to determine the method of tracking system performance over time. The survey should result in a protocol that can guide a round robin evaluation of a system qualification device.

We have begun to construct a radiation transfer standard based on the results of our survey of system usage.[5] A 12.5 mm thick and 30 cm square piece of steel has been prepared for use as an absorber plate, a device to test the resolution of typical systems near their penetration limits. The surface has been ground to eliminate imperfections that could appear as artifacts. The 12.5-mm thickness is appropriate to measure the resolution of the most common system (160 kVp) identified in our survey. The plate will be populated with various image analysis devices in consultation with other members of the task force and after the results of the present survey (tracking performance over time) are available.

We are developing a military standard for radioscopic inspection in a cooperative program with General Electric Company, the U.S. Army Materials Technology Laboratory, and the Naval Air Engineering Center. This standard will list the procedures a military contractor must address before radioscopy can replace radiography in the inspection of military hardware. A draft of this document is now being circulated for comment by domestic users. These comments will be considered for a revision of the draft and the standard will be issued by late 1989. Development of this military standard is being funded by the U.S. Army Materials Technology Laboratory.

References

1. T. A. Siewert, "Standards for Real-Time Radiography - National Bureau of Standards," Proceedings of the Real-Time Imaging III Topical Conference, Cincinnati, Ohio, July 26-28, 1988, to be published by Materials Evaluation (Columbus, Ohio).

2. T. A. Siewert, oral presentation at American Society for Testing and Materials, E07.01 Meeting, Fort Lauderdale, Florida, February 7, 1988.

3. T. A. Siewert, "Improved Standards for Real-Time Radioscopy," Proceedings of 37th Defense Conference on Nondestructive Testing, Jacksonville, Florida, November 1-3, 1988.

4. T. A. Siewert, "Improved Standards for Real-Time Radioscopy," Nondestructive Evaluation: NDE Planning and Application, NDE Vol. 5, Book No. H00468, pp. 95-97 (ASME, 1989).

5. T. A. Siewert, "Typical Usage of Radioscopic Systems: Replies to a Survey," Materials Evaluation 47, p. 701 (June 1989).

6. T. A. Siewert and D. W. Fitting, "An Image Quality Indicator for Radioscopy and Tomography," Review of Progress in Quantitative NDE, Brunswick, Maine, July 23-28, 1989.

Magnetic Methods and Standards for NDE

L. J. Swartzendruber
Metallurgy Division
Institute for Materials Science and Engineering

Magnetic methods are extensively used in nondestructive evaluation. Uses include leakage field detection and measurement to locate and evaluate defects, the measurement of susceptibilities and coercive forces to determine changes in material properties, and Barkhausen noise measurement to determine stress or locate defects. Successful use of these methods requires standardized measurement methods and fundamental knowledge of the relationship between microstructure and magnetic properties.

As recently emphasized by Jiles et al.[1], once properly calibrated, the Barkhausen noise method is capable of unambiguously determining the applied stress, whether in tension or compression. Proper calibration requires both a knowledge of how the noise characteristics change with stress for the particular alloy microstructure being measured, and a knowledge of how the measurement instrument responds to the changes in noise characteristics.

There are several methods for characterization of Barkhausen noise. These methods may be based on, for example, the power density spectrum, the total noise power, the total number of Barkhausen jumps, or the first or second moment of the jump amplitude spectrum. We have developed instrumentation which obtains a complete cycle of noise in digitized form. This information can then be analyzed by digital techniques to obtain all the important noise properties.

A schematic of the equipment being used is shown in Figure 1. The primary additions to the equipment this year are the teslameter and pickup coil. The teslameter is used to measure the tangential component of the magnetic field at the surface of the sample under test. It has been found that this is the most important parameter to utilize when comparing samples with different geometries. Several pickup coils have been developed. In NDE the most important type of coil is a surface coil and two types of surface coils are being used. An equivalent circuit for the sample-coil-preamplifier combination appropriate for both types of coils is shown in Figure 2. The circuit element values must be carefully controlled to obtain reproducible results.

Some typical outputs of Barkhausen noise data are shown in Figure 3. Figure 3a shows the jump amplitudes from an iron foil as the applied field is swept from -30 to +30 Oe. As expected, the peak in the noise output is seen to occur near the coercive force. Also plotted in this figure is the jump amplitude sum which is the integral of the jump amplitudes. Like a hysteresis loop, this curve appears smooth but, as shown by the magnified inset, consists of a series of small jumps. Figure 3b shows the noise power output of the same sample as the field is swept from -30 to +30 Oe, determined by three different

techniques. The widths, heights, and areas of these curves are all important characteristics of the noise. An example of a power density spectrum is shown in Figure 3c, while Figure 3d shows an autocorrelation.

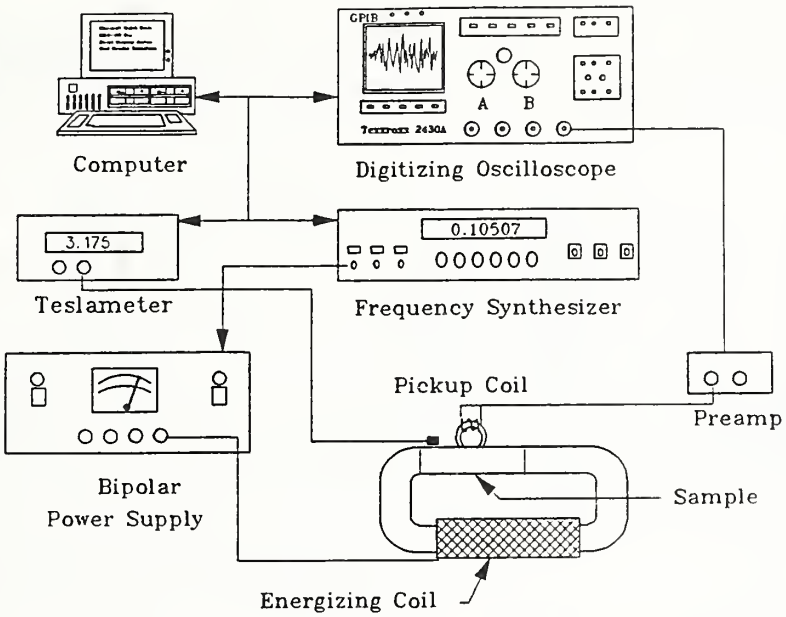

Figure 1. Schematic drawing of the Barkhausen noise apparatus.

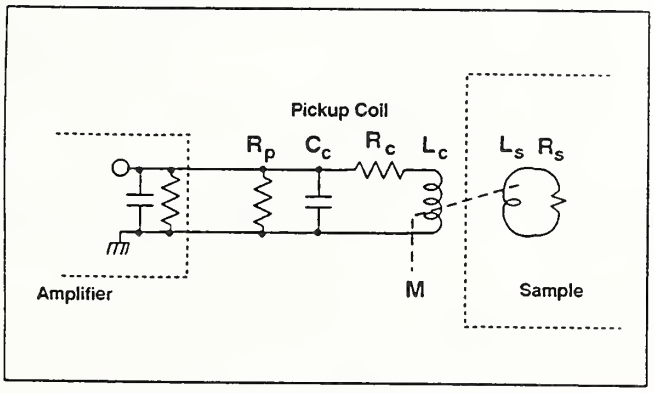

Figure 2. Equivalent circuit for the sample-pickup coil-amplifier.

We plan to utilize the current equipment to characterize a number of samples with various noise characteristics. These samples will then be analyzed on commercially available instruments and their value as calibration standards assessed. Several improvements to the equipment are also planned, including an improved low-noise preamplifier and the use of a 16 bit digitizer. The analysis of noise from a series of well characterized A710 steels and its relation to microstructure and macroscopic properties would also be very useful.

Cooperative work on standards with ASTM Committee E-7 and Committee K of the SAE has continued during the current year. The magnetic particle inspection

standard E 709 is being revised and updated based, in part, on work performed on this project in the past. A new ring standard for use in magnetic particle inspection is being designed. During the coming year it is planned to produce three of the new rings and perform round-robin tests in cooperation with these committees.

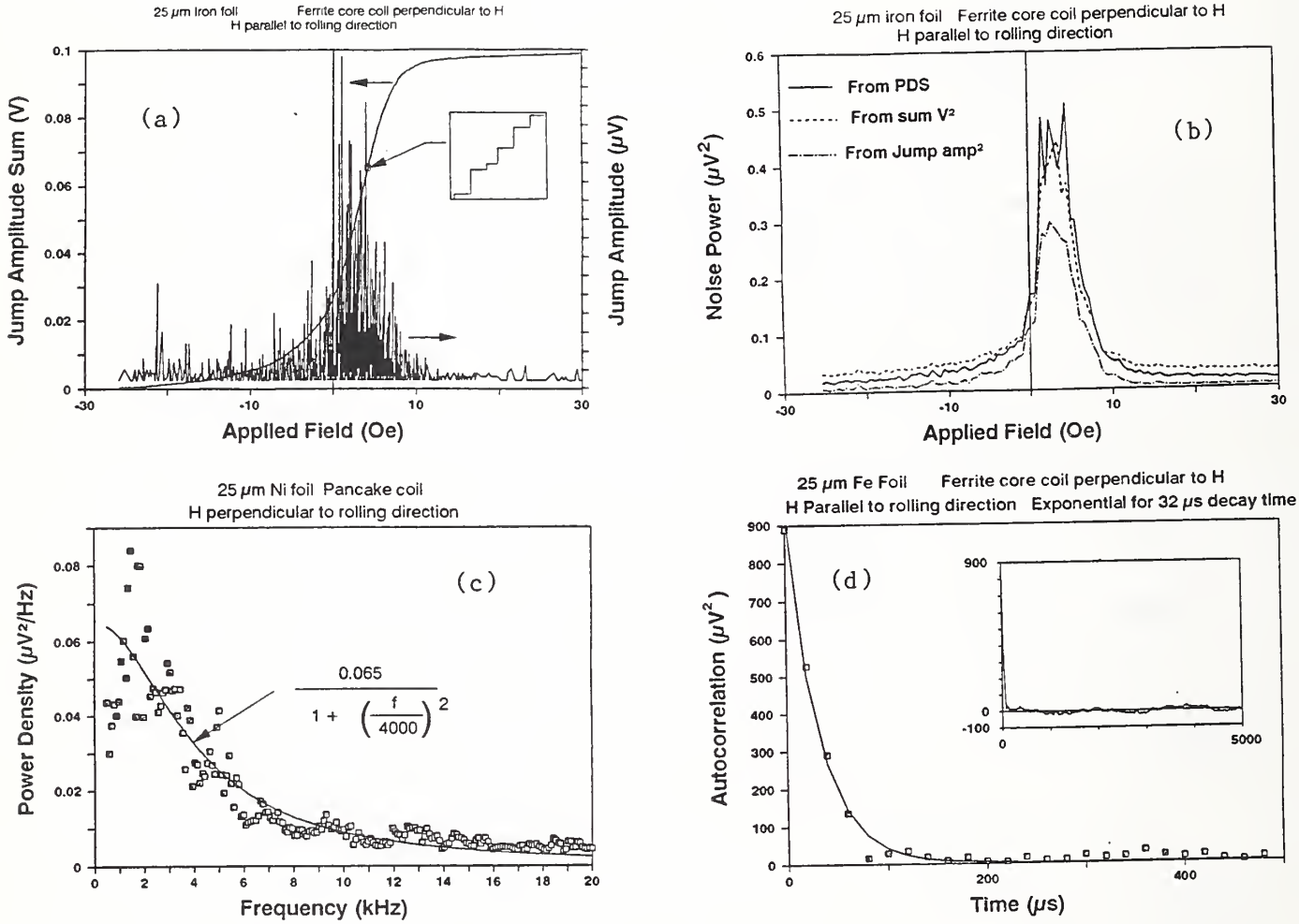

Figure 3. Examples of Barkhausen noise data.

References

1. D. C. Jiles, F. Garikepati, and D. D. Palmer, Review of Progress in Quantitative NDE 8B, p. 2081 (1989).

Eddy Current Techniques

T. E. Capobianco
Electromagnetic Technology Division
Center for Electronics and Electrical Engineering

This program is presently focused on factors affecting the performance of probes used in eddy current nondestructive evaluation inspections and on the

development of techniques and standards for measuring that performance.[1] Eddy current inspections are widely used in both civilian and military applications for finding failure-producing defects in metal parts before they reach critical size. The eddy current technique is a very sensitive method but is affected by many variables. Often these effects are known but not quantified, making the design of equipment or procedures more of an art than a science. We are developing and testing empirical and computer based models of eddy current probe performance so that probe design and selection can be optimized in a predictable fashion.[2]

Coil Construction Factor Study

We are conducting a study of how the physical construction of eddy current coils affects inspection sensitivity. The study design, developed with the help of statisticians from the NIST Center for Applied Mathematics, is based on the statistical concept of multi-dimensional response surface modeling and uses sophisticated software to place design points which will produce the most information with the fewest number of points. Response surfaces can be determined for inspections on high or low conductivity alloys, and for different crack geometries and sizes using a single coil set. In our case, each design point in the study is a coil to be wound and a probe to be built, so efficiency of experimental design is a major consideration.

Table 1 is an updated list of the construction factors and the levels of variations used. In an effort to make the coil winding requirements more manageable, we have divided the set of more than 60 unshielded coils into two parts. The initial group of 26 coils, which is already completed, was chosen from the extremes of the parameter range.

TABLE 1. Construction Factors

Factor	Levels
Ferrite diameter (mm)	0.89, 1.40
Number of turns	90, 120, 180
Winding distance from end (mm)	0.38, 0.76, 1.14
Ferrite permeability	800, 1500, 10,000
Aspect ratio	0.5, 1.0, 2.0
Wire gauge (AWG)	40, 44, 48
Flush cut	True, False

The analysis of this portion of the unshielded coil set has enabled us to identify three factors which are inconsequential, two with weak effects, and two factors with very strong effects. This has allowed us to reduce the size

of the second portion of the set. Presently, we are planning coils to wind, both for the second phase and for the ferrite shielded coil set, based on the results of the first phase of the unshielded coil set. We expect the sensitivity of the shielded coils to be affected by many of the same factors that we are studying now.

To expedite probe construction we wrote a computer program that calculates the physical parameters of the coils such as number of layers, turns per layer, outside diameter and length of the coil from the constraints imposed by each particular combination of construction factor levels such as ferrite diameter, wire gauge, aspect ratio, etc. This has proven very useful and we have modified it for use with air core coils as well.

Air Core Coil Study

The Stanford ΔZ program, which calculates the flaw-induced impedance change of eddy current probes, was installed in August 1988 on the Cyber computer in Boulder by the program's author, Steve Jefferies. Several reruns of previous coil designs were conducted and the program appears to be giving the correct results. While we were planning some coils to wind for an experimental verification of the program results we decided to carry out a study of air core coils analogous to the ferrite core construction factor study. That way, any air core coils wound could be used to validate the construction factor study and the program at the same time. This work is presently underway with most of the computer runs finished, specific coil designs chosen for winding, and the coil and probe construction started.

Flaw Simulations

The NIST Office of Standard Reference Materials reviewed our work last year on the compressed-notch fatigue-crack simulations[3] and funded the production of 100 artifacts midway through this fiscal year. Twenty of these have been delivered, fifty more are in process, and production of an additional thirty is planned for this year. The Department of Commerce has decided to patent the technique and the application is nearly ready for submission to the Patent Office.

In order to simulate a variety of inspection situations for optimizing eddy current probe designs, we have been developing an extensive inventory of well characterized flaws. To date we have made more than ten different EDM notches in 7075-T6 aluminum and have grown four fatigue cracks in the same material. In addition, we have produced eight compressed-notch crack simulations for lab use. We have had some problems controlling size during the growth of fatigue cracks and more work is needed in this area. Future plans call for producing EDM notches in Ti-6Al-4V, and also fatigue cracks when our techniques become more reliable.

Eddy Current Conductivity Apparatus

The conductivity apparatus was shipped to Boulder about a year ago and we have assembled the dc bridge circuitry. These measurements require a closely regulated temperature environment. Unfortunately, the constant temperature bath is

not functioning because of an undetermined electronics problem and a massive tank leak. Obviously, this piece of equipment, which would cost roughly $15K to replace, has become a serious obstacle. In addition, the dc resistance bridge needs a new null detector. As for the ac measurements, the two lock-in amplifiers that came with the apparatus were not functioning when they arrived in Boulder. These were sent out for repair but still do not perform adequately and may need to be replaced. George Free assisted with the assembly and equipment evaluation. He has also been working on the design of a new ac bridge circuit for the apparatus. However, the substantial amount of repair work now required precludes testing of his new circuit until the equipment is brought into working order.

Two Axis Positioner and Data Acquisition System

We have continued our work on the automated eddy current data acquisition apparatus. This system has been used extensively in both the initial and the certification work on the compressed notch fatigue crack simulations, and in both the ferrite and air core construction factor studies. Planned improvements include the addition of a RAM disk for more data handling capacity, which will increase the available scan size, and adding the capability of using differential probes with the system.

References

1. L. L. Dulcie and T. E. Capobianco, "New Standard Test Method for Eddy Current Probes," Proc. of the 36th DoD Conference on NDT (U.S. Army Aviation Systems Command, St. Louis, MO, 1988).

2. T. E. Capobianco and D. F. Vecchia, "Coil Parameter Influence on Eddy Current Probe Sensitivity," Review of Progress in Quantitative NDE 7, p. 487 (1988).

3. T. E. Capobianco, S. J. Ciciora, and J. C. Moulder, "Standard Flaws for Eddy Current Probe Characterization," Review of Progress in Quantitative NDE 8A, p. 985-989 (1989).

New Standard Test Methods for Characterizing Performance of Thermal Imaging Systems

J. Cohen
Consultant
Bethesda, MD

Infrared thermography is being used extensively in industry for nondestructive evaluation and for in-process control, and the applications continue to grow. Thus, there is a demand for new and improved standard test methods that characterize the performance of thermal imaging systems.

The salient characteristics address resolution, detectability, and sensitivity, and we have an ongoing effort to develop the test methods. The first, that for minimum resolvable temperature difference (MRTD), was adopted in late 1987 as

an ASTM standard (E1213-87). The second, for minimum detectable temperature difference (MDTD), is well on the way to adoption.

In FY 1989 work was begun on the third standard test method, that of thermal sensitivity, and designated noise equivalent temperature difference (NETD), the main purpose of which is calibration and periodic monitoring. An overview of the needs and problems in testing was made, from which a preliminary outline of a test method was prepared. Because different types of systems involve different mechanisms of operation, a universal test method is infeasible; thus, the scope of the present work is being confined to FLIR, or scanner, type of systems, where the need is greatest. Further, there is more than one possible method for obtaining the performance measure, so an assessment is in progress to determine the best one based on precision and accuracy. Future work will examine a means for standardizing and defining the noise bandwidth, without which NETD would be meaningless.

Capacitive Array Research for Characterization of Ceramics

P. J. Shull, A. V. Clark, V. Tewary, and D. V. Mitrakovic*
Fracture and Deformation Division
Institute for Materials Science and Engineering

*Guest Worker from the University of Belgrade, Yugoslavia

A promising technique for process monitoring in ceramic manufacture is measurement of the material's dielectric constant. In the laboratory, this can be accomplished by measuring the capacitance of a parallel plate capacitor with the material placed between the plates. In industrial practice, it is much more likely that access to the ceramic can be had from one side only.

Hence, we are exploring the use of a capacitive probe that consists of an array of electrodes lying in the same plane. When a voltage is impressed on the electrodes, the resultant electric field "fringes" into the space in front of the electrodes. The electric field will be perturbed by the presence of any dielectric material in the vicinity.

Our initial system design can be represented by the equivalent circuit of Figure 1. Here, half the electrodes are connected to a voltage source; these are "source" electrodes. The other half are connected to a device which measures the current, I_{out}; these are indicated by "receiver". The probe capacitance, C, is obtained from: $C = I_{out}/\omega V_0$ where ω = frequency of voltage source.

An elementary theory[1] can be used to predict the change, ΔC, in probe capacitance when a dielectric material of permittivity, ϵ, is placed at a distance, d, from the probe:

$$\Delta C = \frac{1}{\left(\frac{\epsilon+\epsilon_o}{\epsilon-\epsilon_o}\right) e^{2ad} - 1} \qquad (1)$$

where ϵ_o = permittivity of free space. In deriving equation (1), the following assumptions are made: a) the dielectric material is a half-space; b) the probe is of infinite extent; c) the probe potential varies sinusoidally, with spatial frequency, a.

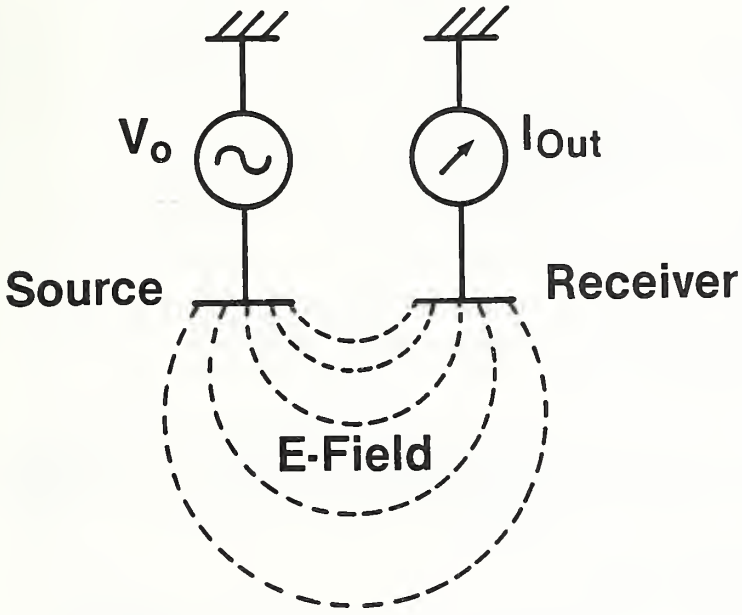

Figure 1. Schematic of unbalanced system used in initial experiments to test validity of theory of Ref. 1.

For contact operation (d = 0), it is then theoretically straightforward to obtain ϵ.. However, there are cases where noncontact operation may be necessary, such as in sintering of superconducting ceramics. For these noncontact applications, means must be found to obtain ϵ when the liftoff, d, is unknown.

One obvious method is to vary the spatial frequency, a. We can approximate this by varying the pattern of potential on the electrodes. For example, we may have a potential, $+V_0$, on even-numbered electrodes, and $-V_0$ on odd-numbered electrodes. Then, we may change the pattern so that even pairs of electrodes are at $+V_0$, and odd pairs are at $-V_0$, and so on. By varying a, with d fixed, we can obtain an overdetermined set of equations for $\Delta C(a,d,\epsilon)$ that can be solved, for example, by nonlinear least squares methods to find ϵ and d.

A necessary condition for this method to work is that the theory of equation (1) be valid. One test of the theory is to vary d on specimens of known ϵ, and compare measured ΔC with the predictions of the equation. In particular, the theory predicts a monotonic decrease of ΔC with liftoff.

We previously reported the results of our experiments, which were at variance with the theory. The results of numerous experiments we have performed can be summarized by Figure 2, where an initial decrease in amplitude is followed by a "recovery".[2,3] (The amplitude is proportional to ΔC.)

We have now identified the source of this anomaly. The circuit of Figure 1 essentially ties all receiver electrodes to ground (zero potential). Thus, the probe is not balanced; the average voltage is $V_0/2$, and not zero as would be

required for a sinusoidal potential pattern. The non-zero component causes the probe to act as one plate of a capacitor, with an electric field which links to any conductors in the environment. We have shown both theoretically and experimentally that this linkage (parasitic capacitance) is the cause of the "recovery" effect of Figure 2.

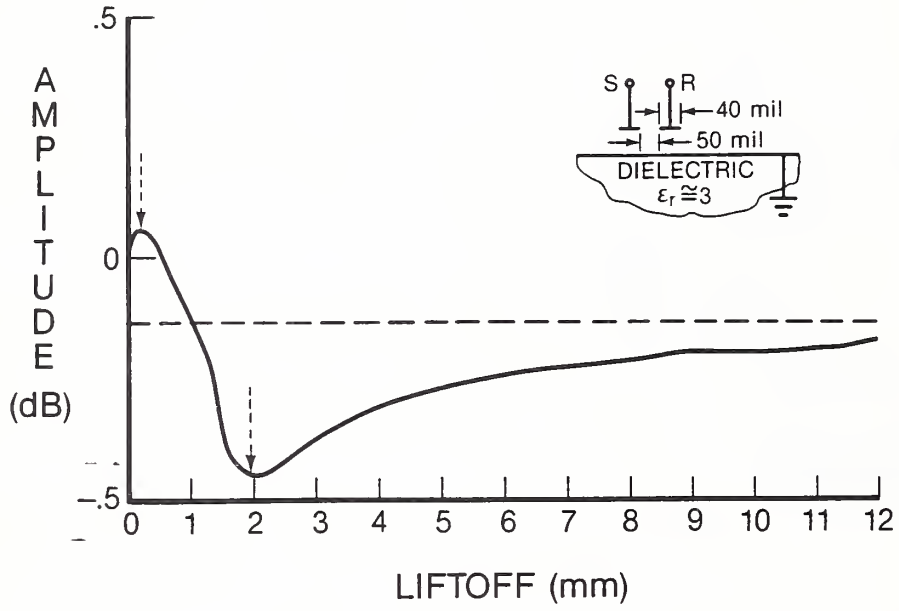

Figure 2. Typical result of experiments performed with unbalanced system. Note initial decrease, followed by "recovery".

We have built a balanced circuit which is shown in Figure 3.[4] Here, the potential difference across source ("S") and receiver ("R") electrodes is V_0, but the average voltage is zero. The probe admittance is very small (typically $5 \times 10^{-6}\ \Omega^{-1}$), so it is necessary to have high-impedance buffer amplifiers, A_{ref} and A_p to force the current to flow through the capacitances and not enter the differential amplifier. The buffer amplifiers respond to the voltage drops, ωRCV_0, across the precision resistors, R_{ref} and R_p, where $R_{ref} = R_p$. The output voltage, V_{out}, is proportional to the difference between C_p and C_{ref}, with C_p = probe capacitance, C_{ref} = reference capacitance. To avoid dynamic range problems, we trim C_{ref} so that $C_{ref} = C_p$ in the absence of the specimen. Because the currents are typically in the μA range, low-noise components must be used in the circuit.

We repeated our previous measurements, but now using our balanced system. A typical result is shown in Figure 4, which indicates that the "recovery" artifact has been suppressed.

As mentioned previously, it is theoretically straightforward to obtain ϵ from equation (1) for contact measurements ($ad \to 0$). Such measurements are useful, for example, for high-ϵ materials. In this case, $\partial \Delta C / \partial \epsilon$ becomes small (unless $ad \ll 1$) and we lose sensitivity to ϵ. In effect, the high polarizability of the material shields the interior of the specimen from the probe field, unless

the probe is very near the surface. In the latter case, some of the field is forced into the material, and sensitivity is recovered.

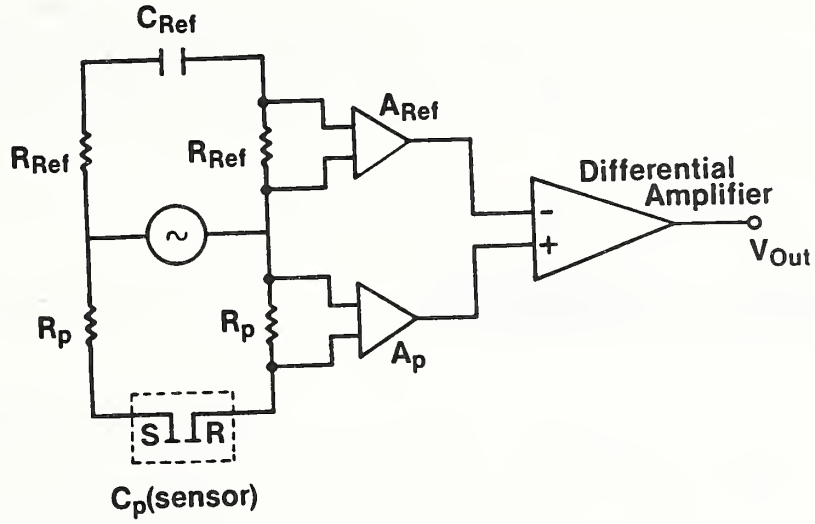

Figure 3. Schematic of balanced system developed to suppress parasitic capacitive coupling to environment.

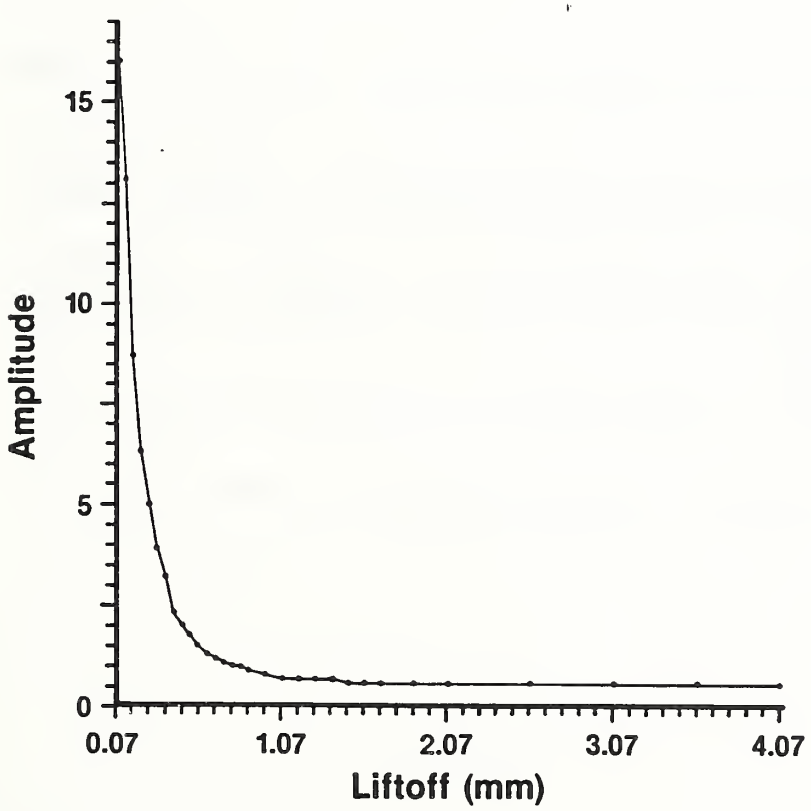

Figure 4. Typical result of experiments performed with balanced system. Note monotonic decrease, with no "recovery".

However, we expect that the theory of equation (1) will not be valid for the actual situation pertaining in contact operation. In particular, the theory

assumes that the probe electrodes exist everywhere (are continuous); in fact, the electrodes are discrete, and finite in number.

We have developed a theory to model the finite electrode case. We use strip electrodes in our experiments, which allows us to model the problem as two-dimensional. We solve Laplace's equation for the (electrostatic) potential field Φ: $\nabla^2\Phi = 0$. We use functions of a complex variable, z, of the form:

$$\Phi = f(z) + \left(\frac{1-\epsilon}{1+\epsilon}\right) f(z+2d) \quad \text{(above specimen)}$$

$$\Phi = \left(\frac{2}{1+\epsilon}\right) f(z) \quad \text{(in specimen)}$$

This automatically satisfies continuity conditions at the specimen surface. The functional form of f(z) is chosen to give the correct potential at the discrete electrodes.[5] The solution has been verified by showing that it gives good agreement with values of Φ calculated with a finite element model. We will use our solution to perform a parametric study of the effect of ϵ and d on the capacitance of an array of discrete electrodes.

References

1. M. Gimple, "Capacitive Arrays for Robotic Sensing," Ph.D. Thesis, Stanford University, 1988.

2. P. J. Shull, A. V. Clark and P. R. Heyliger, "Liftoff: Capacitive Array Sensors," Rev. of Progress in Quantitative NDE 8A, pp. 1013-1021 (1988).

3. P. J. Shull, A. V. Clark, Paul Heyliger, B. A. Auld, and J. C. Moulder, "Characterization of Capacitive Array for NDE," submitted to Research in Nondestructive Evaluation.

4. P. J. Shull, A. V. Clark, V. Tewary, and D. V. Mitrakovic, manuscript in preparation.

5. V. Tewary, A. V. Clark, and P. J. Shull, manuscript in preparation.

PERSONNEL

PERSONNEL

The permanent staff of the Office of Nondestructive Evaluation is listed in the Table below. This staff was supplemented on a part-time basis during FY 1989 by Dr. Andrew J. Buechele, a contract scientist from the Catholic University of America.

TABLE I. STAFF

ONDE PERMANENT STAFF IN FISCAL YEAR 1989
H. Thomas Yolken, Chief
Leonard Mordfin, Deputy Chief
George Birnbaum, Senior Scientist
Patty Salpino, Administrative Officer
Joan Fravel, Secretary
Linda Souders, Secretary

Although ONDE has a small staff, the Office is able to work effectively in its program management role. ONDE helps to identify and recruit guest scientists, research associates, and other temporary participants in the Program. This is an effective means for strengthening the Program's research staff, bringing in fresh ideas and new approaches, and disseminating the research results. ONDE provides partial support for some of these temporaries.

Among the temporary participants in the Program who received support from ONDE in FY 1989 are Hanania Ettedgui and Yitzhak Grinberg, guest scientists from the Nuclear Research Center Negev in Israel. Ettedgui worked with Dr. Lydon Swartzendruber of the Metallurgy Division on magnetic NDE methods, and Grinberg is working with Dr. Ward Johnson, also of the Metallurgy Division, on ultrasonic inspection of hot metals. Dr. Xuan Tong Ying, a guest scientist from Fudan University in the Peoples Republic of China, works with Dr. Albert Feldman of the Ceramics Division on thermal wave tests of diamond films and Mr. Shuchu Ren, a guest scientist from the Institute of Acoustics, Chinese Academy of Sciences, Beijing, Peoples Republic of China, works with Dr. Nelson Hsu of the Automated Production Technology Division on ultrasonic propagation in composites and interfaces. Three retired NIST employees, all of whom had participated in the NDE Program, have returned on a part-time basis in the Program: Dr. Hans Frederikse works with Dr. Feldman on the diamond film project and with Dr. Thomas Lettieri of the Precision Engineering Division on infrared inspection of solder joints; Dr. Robert Placious is drafting a military standard on measurement of visual acuity in the Ionizing Radiation Division; and Julius Cohen is drafting an ASTM standard on performance criteria for thermographic equipment.

The NDE expertise and facilities, which are developed in the divisions that participate in the NDE Program, attract industrial research associates to those divisions. Research associates obviously constitute a major vehicle for transferring the NIST's NDE results to industry; at the same time they generally contribute to the success of the NDE projects as well. One such research associate in the NDE Program is Mr. Mike Mester from the Aluminum Association who works with Dr. Arnold Kahn in the Metallurgy Division on the development of eddy current sensors for aluminum processing. Mr. Tom Lizzi of Crucible Materials and Mr. James Ingram of Hoeganaes participate in the metal powder atomization project via the industrial research consortium that ONDE initiated in 1987.

OUTPUTS AND INTERACTIONS

OUTPUTS AND INTERACTIONS

A. NDE SEMINARS AT NIST

Dr. Bernhard R. Tittmann, Rockwell International Science Center
"Elastic Anisotropy in Composites"
December 5, 1988

Dr. Chris M. Fortunko, ElectroSonics
"Nonconventional Ultrasonic Instrumentation and Methods in Nondestructive Evaluation of Composite Materials and Structures"
February 15, 1989

Dr. Christopher Woods and colleagues, Harwell - United Kingdom
"Description of NDE Research and Services"
April 6, 1989

Dr. A. C. Boccaro, Ecole Supérieure de Physique et de Chimie Industrielles, Paris, France
"Photothermal Techniques: From Technology to Basic Physics"
August 4, 1989

Dr. G. Jiang, Research Institute of Electric Light Source Materials, Peoples Republic of China
"Intelligent Sensors for Atomization Processing of Molten Metals and Alloys"
August 28, 1989

B. INVITED TALKS BY ONDE STAFF

"Intelligent Processing of Materials," H. T. Yolken, National Materials Advisory Board, National Academy of Sciences, Washington, D.C., January 10, 1989.

"Introduction to Laser Techniques in NDE," G. Birnbaum, 1989 ASNT Spring Conference, Charlotte, North Carolina, March 22, 1989.

"Overview of the Nondestructive Evaluation Program at NIST," L. Mordfin and G. Birnbaum, OSTP/COMAT Ad Hoc Working Group on Nondestructive Evaluation, Alexandria, Virginia, May 15, 1989.

"Intelligent Processing of Materials," H. T. Yolken, Fifth Scandinavian Symposium on Materials Science, Copenhagen, Denmark, May 24, 1989.

"Intelligent Processing of Materials--The Role of Sensors," H. T. Yolken, 4th NIST/BAM Symposium, Gaithersburg, Maryland, September 28, 1989.

C. PUBLICATIONS

Following is an incomplete listing of NIST reports and publications on NDE and related topics that have become available since last year's Technical Activities report was prepared. Included are several publications that were inadvertently omitted from last year's compilation.

Anon., "'HIPing': From Metal Powders to Reliable Materials," NIST Research Reports, NIST SP 765, pp. 12-13 (June 1989).

Anon., "NIST/Industrial Consortium on Automated Processing of Rapidly Solidified Metal Powders by High Pressure Inert Gas Atomization, Second Annual Report, Aug. 1, 1988 - July 31, 1989," 63 pp. (1989; limited distribution).

B. A. Auld, J. C. Moulder, S. Jefferies, P. J. Shull, S. Ayter, and J. Kenney, "Eddy-Current Reflection Probes: Theory and Experiment," Research in Nondestructive Evaluation 1, No.1, pp. 1-11 (1989).

R. Berliner, H. G. Smith, J. R. D. Copley, and J. Trivisonno, "Neutron Diffraction Studies of the Martensitic Transformation in Sodium Metal," NBS Reactor: Summary of Activities July 1987 Through June 1988, NIST TN 1257, pp. 69-70 (Jan. 1989).

G. V. Blessing and D. G. Eitzen, "Surface Roughness Sensed by Ultrasound," Surface Topography 1, pp. 253-267 (1988).

G. V. Blessing and D. G. Eitzen, "Surface Roughness Monitored with an Ultrasonic Sensor," Technical Paper MS89-431-1-7 (Soc. Mfg. Engrs., 1989).

F. R. Breckenridge, T. M. Proctor, N. N. Hsu, S. E. Fick, and D. G. Eitzen, "Ultrasonic Measurements Research: Progress in 1988," Report No. AD A20113 (Defense Documentation Center, 1988).

A. J. Bur, F. W. Wang, A. Lee, R. E. Lowry, S. C. Roth, and T. K. Trout, "In Situ Fluorescence Monitoring of the Viscosities of Particle-Filled Polymers in Flow," NISTIR 88-3892, 36 pp. (Nov. 1988).

T. E. Capobianco, S. J. Ciciora, and J. C. Moulder, "Standard Flaws for Eddy Current Probe Characterization, Review of Progress in Quantitative NDE 8A, pp. 985-989 (1989).

K. H. Cavcey, "Transmission Loss Through 6061 T-6 Aluminum Using a Pulsed Eddy Current Source," Materials Evaluation 47, No. 2, pp. 216-218 (Feb. 1989).

Y. T. Cheng, M. J. Blackman, J. S. Olin, and M. Ganoczy, "The Smithsonian - NBS Program on the Studying of Art Objects by Neutron Methods," NBS Reactor: Summary of Activities July 1987 Through June 1988, NIST TN 1257, pp. 152-156 (Jan. '89).

C. S. Choi and H. J. Prask, "Neutron Diffraction Study of Textures of Materials," NBS Reactor: Summary of Activities July 1987 Through June 1988, NIST TN 1257, pp. 77-81 (Jan. 1989).

A. V. Clark, R. B. Thompson, G. V. Blessing, and D. Matlock, "Ultrasonic Measurement of Formability in Thin Ferritic Steel Sheet," Review of Progress in Quantitative NDE 8A, pp. 1031-1038 (1989).

A. V. Clark, R. B. Thompson, R. C. Reno, G. V. Blessing, and D. Matlock, "Steel Stamping Technology: Applications and Impact," Paper SP-779 (Soc. Auto. Engrs., 1989).

J. Cohen, "Fundamentals and Applications of Infrared Thermography for Nondestructive Testing," International Advances in Nondestructive Testing 13, pp. 39-81, (Gordon & Breach, New York, 1988).

J. R. D. Copley, "The Significance of Multiple Scattering in the Interpretation of Small Angle Neutron Scattering Experiments," NBS Reactor: Summary of Activities July 1987 Through June 1988, NIST TN 1257, pp. 94-96 (Jan. 1989).

S. Datta, H. Ledbetter, and T. Kyono, "Graphite Fiber Elastic Constants: Determination from Ultrasonic Measurements on Composite Materials," Review of Progress in Quantitative NDE 8B, pp. 1481-1488 (1989).

P. Dutta, G. A. Candela, D. Chandler-Horowitz, J. F. Marchiando, and M. C. Peckerar, "Nondestructive Characterization of Oxygen-Ion-Implanted Silicon-on-Insulator Using Multiple-Angle Ellipsometry," Applied Physics Letters 64, No. 5, pp. 2754-2756 (Sept. 1, 1988).

R. J. Fields, E. N. Pugh, D. T. Read, J. H. Smith, "An Assessment of the Performance and Reliability of Older ERW Pipelines," NISTIR 89-4136 (July 1989).

D. W. Fitting, R. D. Kriz, and A. V. Clark, Jr., "Measuring In-Plane Elastic Moduli of Composites with Arrays of Phase-Sensitive Ultrasound Receivers," Review of Progress in Quantitative NDE 8B, pp. 1497-1504 (1989).

H. P. R. Frederikse and X. T. Ying, "Heat Conductivity of Oxide Coatings by Photothermal Radiometry Between 293 and 1173 K," Applied Optics 27, No. 2, pp. 4672-4675 (1988).

R. G. Geyer, "Magnetostatic Measurements for Mine Detection," NISTIR 88-3098 (Oct. 1988).

P. R. Heyliger, J. C. Moulder, and N. Nakagawa, "Numerical Simulation of Flaw Detection with a Capacitive Array Sensor Using Finite and Infinite Elements," Review of Progress in Quantitative NDE 8A, pp. 1023-1030 (1989).

D. A. Hill, "Electromagnetic Scattering by Buried Objects of Low Contrast," IEEE Transactions on Geoscience and Remote Sensing 26, No. 2, pp. 195-203 (March 1988).

N. N. Hsu and D. G. Eitzen, "Higher-Order Crossings -- A New Acoustic Emission Signal Processing Method," Progress in Acoustic Emissions IV, pp. 59-66 (Japanese Society for NDI, 1988).

R. D. Kriz and P. R. Heyliger, "Finite Element Model of Stress Wave Topology in Unidirectional Graphite/Epoxy: Wave Velocities and Flux Deviations," Review of Progress in Quantitative NDE 8A, pp. 141-148 (1989).

C. Lin and Tinh Nguyen, "An Electrochemical Technique for Rapidly Evaluating Protective Coatings on Metals," NIST Technical Note 1253, 23 pp. (Oct. 1988).

R. G. Mathey and J. R. Clifton, "Review of Nondestructive Evaluation Methods Applicable to Construction Materials and Structures, NBS TN 1247, 203 pp. (June 1988).

F. McGehan, "'Standard Crack' Helps Detect Metal Fatigue in Aircraft," NIST Research Reports, NIST SP 765, p. 9 (June 1989).

A. Moini, M. S. Wang, T. J. Pinnavaia, and D. A. Neumann, "Studies on the Dispersion of Clay Particles in Epoxy by Small-Angle Neutron Scattering," NBS Reactor: Summary of Activities July 1987 Through June 1988, NIST TN 1257, pp. 18-21 (Jan. 1989).

F. I. Mopsik, E. F. Kelley, and F. D. Martzloff, "A Review of Candidate Methods for Detecting Incipient Defects Due to Aging of Installed Cables in Nuclear Power Plants, NBSIR 88-3774 (May 1988).

F. I. Mopsik, S.-S. Chang, and D. L. Hunston, "Dielectric Measurements for Cure Monitoring," Materials Evaluation 47, pp. 448-453 & 455 (April 1989).

L. Mordfin, "NDE Publications: 1985," NISTIR 89-4131, 42 pp. (Aug. 1989).

L. Mordfin and G. Birnbaum, "NIST Presentation," Summary Record of the 1989 Meeting of the Ad Hoc Working Group on Nondestructive Evaluation (NDE), Office of Science and Technology Policy (OSTP)/Committee on Materials (COMAT), R. T. Loda, editor, IDA Document D-612, pp. 17-34 (Institute for Defense Analyses, Alexandria, VA, June 1989).

Tinh Nguyen and C. D. Olson, "Application of Thermal-Wave Electron Microscopy to Imaging and Assessment of Corrosion on Rough Steel Surface," Materials and Structures 22, pp. 71-79 (1989).

S. P. Pessiki and N. J. Carino, "Setting Time and Strength of Concrete Using the Impact-Echo Method," ACI Materials Journal 85, No. 5, pp. 389-399 (American Concrete Institute, Sept.-Oct. 1988).

C. Presser, A. K. Gupta, and H. G. Semerjian, "Dynamics of Pressure-Jet and Air-Assist Nozzle Sprays: Aerodynamic Effects," Paper No. AIAA-88-3139 (Am. Inst. Aeronautics & Astronautics, New York, 1988).

C. Presser, F. Biancaniello, S. D. Ridder, and H. G. Semerjian, "Laser Diffraction Measurements in an Inert-Gas Metal Atomizer," Proc. 3rd Annual Conf. on Liquid Metal Atomization and Spray Systems (ILASS Americas '89), pp. 166-170 (1989).

T. M. Proctor, "Transducer for Measuring Transient Tangential Motion," U. S. Patent No. 4,782,701 (Nov. 8, 1988).

T. M. Proctor, "A High Fidelity Piezoelectric Tangential Displacement Transducer for Acoustic Emission," J. Acoustic Emission 7, No. 1, pp. 41-48 (1988).
S. Ren, N. N. Hsu, and D. G. Eitzen, "Transient Green's Tensors for a Layered Solid Half-Space with Different Interface Conditions," J. Acoust. Soc. Am. 83, Suppl. 1, p. S20 (1988).

R. Rensberger, "Building Quality into Advanced Materials during Processing," NIST Research Reports, NIST SP 765, pp. 10-11 (June 1989).

S. D. Ridder and F. S. Biancaniello, "Process Control During High Pressure Atomization," Mat. Sci. Engrg. 98, pp. 47-51 (1988).

M. Sansalone and N. J. Carino, "Impact-Echo Method," Concrete International: Design and Construction, 9 pp. (American Concrete Institute, April 1988).

M. Sansalone and N. J. Carino, "Laboratory and Field Studies of the Impact-Echo Method for Flaw Detection in Concrete," Nondestructive Testing, SP-112, H. S. Lew, editor, pp. 1-20 (American Concrete Institute).

M. Sansalone and N. J. Carino, "Detecting Delaminations in Concrete Slabs with and without Overlays Using the Impact-Echo Method," ACI Materials Journal 86, No. 2, pp. 175-184 (American Concrete Institute, March-April 1989).

R. E. Schramm, P. J. Shull, A. V. Clark, Jr., and D. V. Mitrakovic, "EMATs for Roll-By Inspection of Railroad Wheels," Review of Progress in Quantitative NDE 8A, pp. 1083-1089 (1989).

P. J. Shull, A. V. Clark, and P. R. Heyliger, "Liftoff: Capacitive Array Sensors," Review of Progress in Quantitative NDE 8A, pp. 1013-1021 (1988).

T. A. Siewert, "Typical Usage of Radioscopic Systems: Replies to a Survey," Materials Evaluation 47, pp. 701-705 (June 1989).

T. A. Siewert, "Improved Standards for Real-Time Radioscopy," Nondestructive Evaluation: NDE Planning and Application, NDE Vol. 5, Book No. H00468, pp. 95-97 (ASME, 1989).

L. J. Swartzendruber, "Quantitative Problems in Magnetic Particle Inspection," Review of Progress in Quantitative NDE 8B, pp. 2133-2140 (1989).

[L. J. Swartzendruber], "Military Standard: Inspection, Magnetic Particle," MIL-STD-1949A, 28 pp. (15 May 1989).

H. N. G. Wadley, J. A. Simmons, and E. Drescher-Krasicka, "Ultrasonic Propagation at Metal-Ceramic Interfaces in Composites," Materials Research Soc. Symposium Proceedings 120, pp. 341-350 (1988).

A. Wolfenden, M. R. Harmouche, G. V. Blessing, Y. T. Chen, P. Terranova, V. Dayal, V. K. Kinra, J. W. Lemmens, R. R. Phillips, J. S. Smith, P. Mahmoodi, and R. J. Wann, "Dynamic Young's Modulus Measurements in Metallic Materials: Results of an Interlaboratory Testing Program," ASTM J. Testing & Evaluation 17, No. 1, pp. 2-13 (Jan. 1989).

H. T. Yolken, editor, "Nondestructive Evaluation - Technical Activities - 1988," NISTIR 88-3839, 73 pp. (Oct. 1988).

H. T. Yolken, editor-in-chief, Research in Nondestructive Evaluation 1 (ASNT/Springer International, 1989).

H. T. Yolken and L. Mordfin, "Intelligent Processing of Materials - Report of an Industrial Workshop Conducted by the National Institute of Standards and Technology," NISTIR 89-4024, 50 pp. (Jan. 1989).

D. AWARDS AND APPOINTMENTS

Department of Commerce Gold Medal

The Gold Medal Award for Distinguished Service, the Department of Commerce's highest honor award, is bestowed for distinguished achievements of major significance to the Department or the nation. Arnold H. Kahn of the Metallurgy Division, a principal investigator in the NDE Program, was honored with a gold medal for his theoretical studies of electromagnetic interactions with metallic materials, which pioneered the measurement basis for sensors to determine internal temperature and dimensions of alloys undergoing metalforming processes.

McKay-Helm Award

The American Welding Society named Thomas A. Siewert a co-recipient of its McKay-Helm Award and the Honorary Membership Award. The McKay-Helm Award honors the best papers published in the Welding Journal. Dr. Siewert, who serves as the NDE Program's principal investigator for x-ray radiology, is a metallurgist in the Fracture and Deformation Division.

Department of Commerce Silver Medal

The Silver Medal Award for Meritorious Service, which is the second highest honor awarded by the Department of Commerce, is bestowed for meritorious contributions of exceptional value to the Department. In recognition of his contributions to the development of sensors and their integration into automated control systems for materials processing, a silver medal was granted to Haydn N. G. Wadley. A metallurgist, Dr. Wadley served until recently as the leader of the Advanced Sensors Group in the Metallurgy Division.

ASTM Award of Merit

An ASTM Award of Merit and the title of Fellow of the Society were awarded to Leonard Mordfin of the Office of Nondestructive Evaluation. Dr. Mordfin was

cited for distinguished leadership and exceptional contributions in the promotion, development, and the growth of the ASTM committee on mechanical testing.

Department of Commerce Bronze Medal

The Bronze Medal Award for Superior Federal Service is the highest honorary recognition available for NIST presentation. This year's recipients included John E. Blendell of the Ceramics Division and Stephen D. Ridder of the Metallurgy Division, both of whom are principal investigators in the NDE Program. Dr. Blendell was recognized for his leadership in the development of a capability for processing high-temperature superconductors, and Dr. Ridder was honored for his outstanding contributions to the study of atomization processes in metals.

H. Thomas Yolken, Office of Nondestructive Evaluation, was appointed editor-in-chief of ASNT's new journal, Research in Nondestructive Evaluation.

George Birnbaum, Office of Nondestructive Evaluation, was appointed research professor in the Physics Department of The Catholic University of America.

APPENDICES

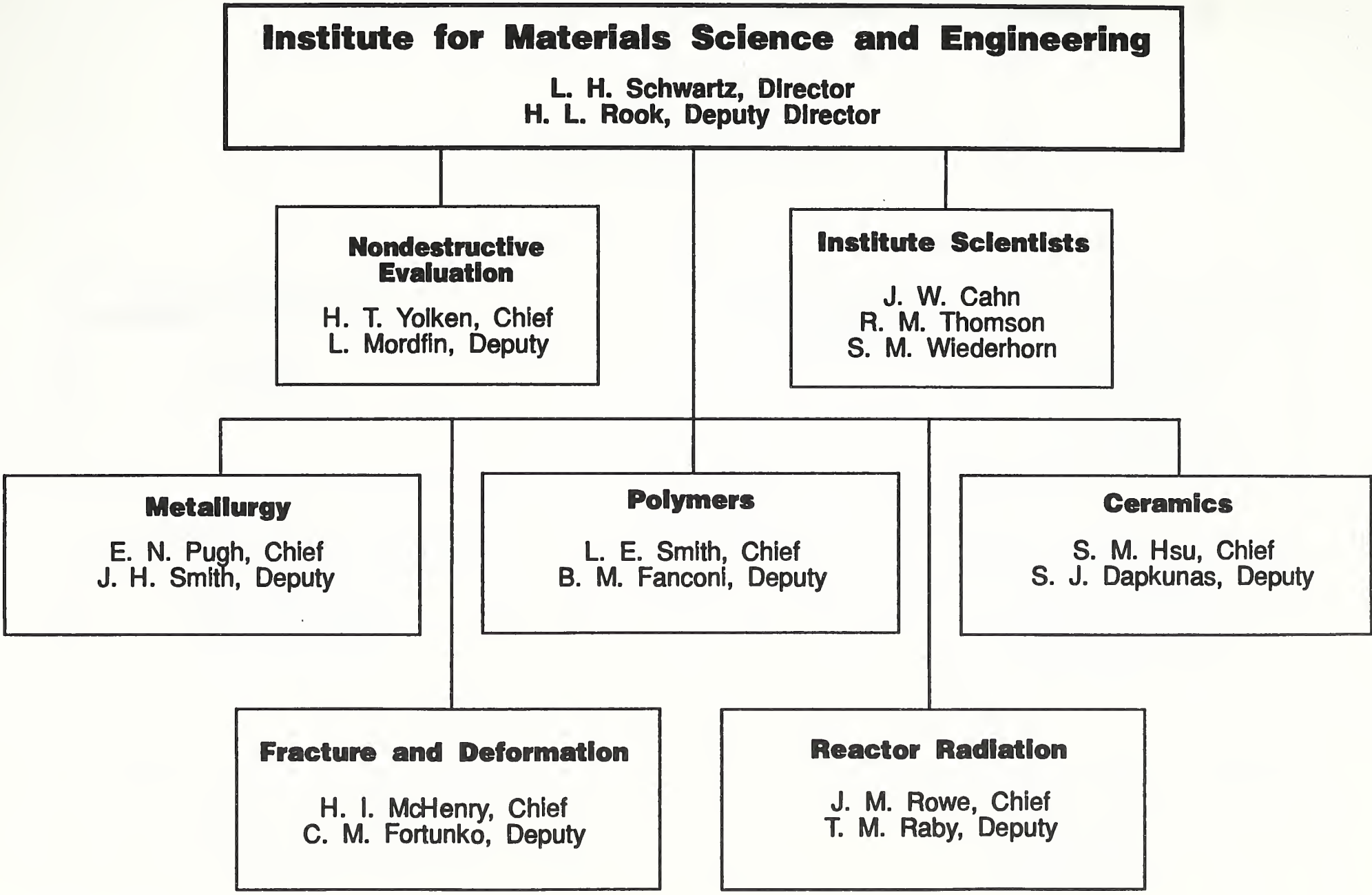
Institute for Materials Science and Engineering
L. H. Schwartz, Director
H. L. Rook, Deputy Director
Nondestructive Evaluation
H. T. Yolken, Chief
L. Mordfin, Deputy
Institute Scientists
J. W. Cahn
R. M. Thomson
S. M. Wiederhorn
Metallurgy
E. N. Pugh, Chief
J. H. Smith, Deputy
Polymers
L. E. Smith, Chief
B. M. Fanconi, Deputy
Ceramics
S. M. Hsu, Chief
S. J. Dapkunas, Deputy
Fracture and Deformation
H. I. McHenry, Chief
C. M. Fortunko, Deputy
Reactor Radiation
J. M. Rowe, Chief
T. M. Raby, Deputy

U.S. DEPARTMENT OF COMMERCE
National Institute of Standards and Technology

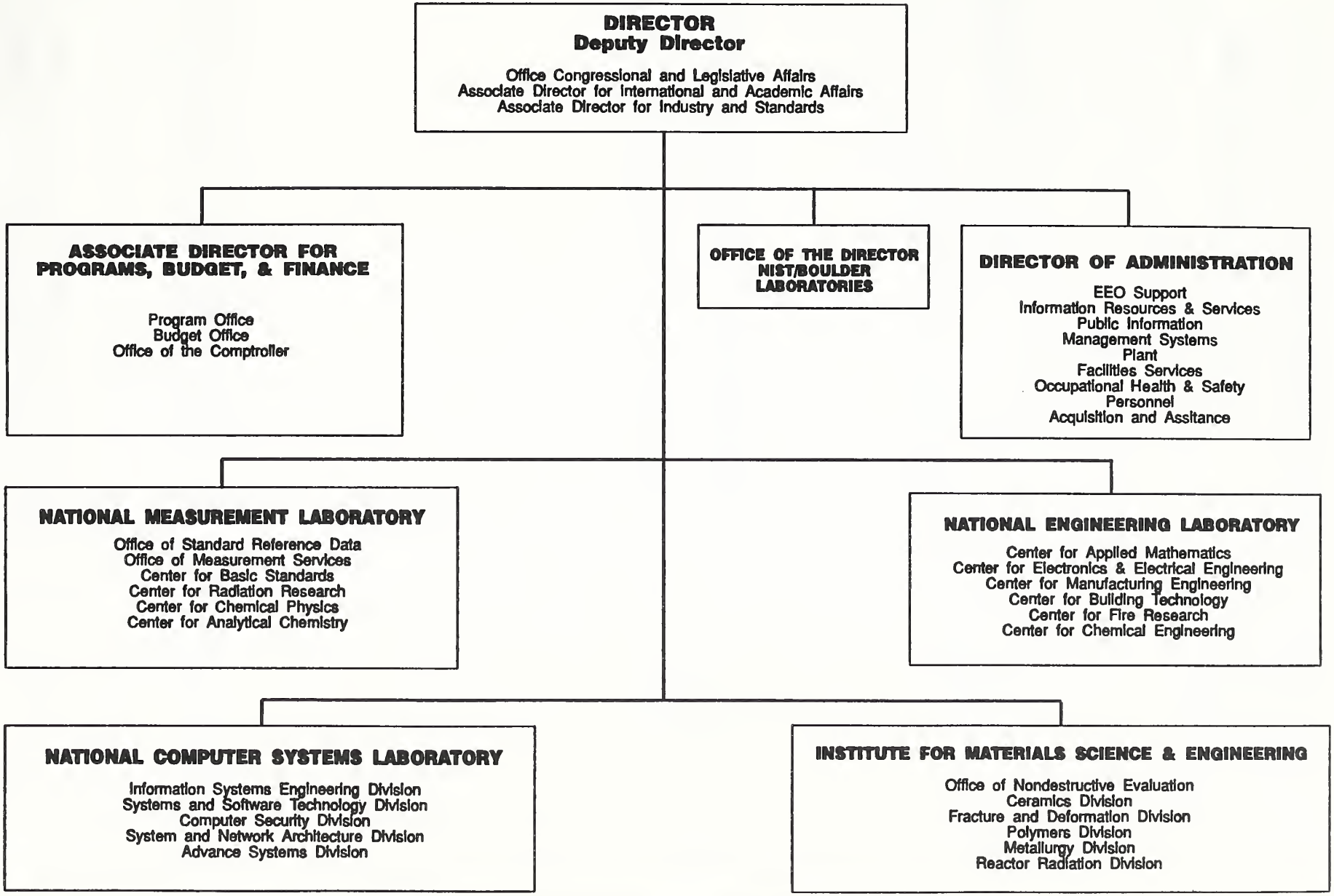

NIST-114A
(REV. 3-89)

U.S. DEPARTMENT OF COMMERCE
NATIONAL INSTITUTE OF STANDARDS AND TECHNOLOGY

BIBLIOGRAPHIC DATA SHEET

1. PUBLICATION OR REPORT NUMBER
NISTIR 89-4147

2. PERFORMING ORGANIZATION REPORT NUMBER

3. PUBLICATION DATE
NOVEMBER 1989

4. TITLE AND SUBTITLE

Technical Activities 1989--Nondestructive Evaluation

5. AUTHOR(S)

H. Thomas Yolken, editor

6. PERFORMING ORGANIZATION (IF JOINT OR OTHER THAN NIST, SEE INSTRUCTIONS)

U.S. DEPARTMENT OF COMMERCE
NATIONAL INSTITUTE OF STANDARDS AND TECHNOLOGY
GAITHERSBURG, MD 20899

7. CONTRACT/GRANT NUMBER

8. TYPE OF REPORT AND PERIOD COVERED
Annual, FY89

9. SPONSORING ORGANIZATION NAME AND COMPLETE ADDRESS (STREET, CITY, STATE, ZIP)

National Institute of Standards and Technology
U.S. Department of Commerce
Gaithersburg, MD 20899

10. SUPPLEMENTARY NOTES

[ ] DOCUMENT DESCRIBES A COMPUTER PROGRAM; SF-185, FIPS SOFTWARE SUMMARY, IS ATTACHED.

11. ABSTRACT (A 200-WORD OR LESS FACTUAL SUMMARY OF MOST SIGNIFICANT INFORMATION. IF DOCUMENT INCLUDES A SIGNIFICANT BIBLIOGRAPHY OR LITERATURE SURVEY, MENTION IT HERE.)

A review of the Nondestructive Evaluation Program at NIST for fiscal year 1989 is presented in this annual report.

12. KEY WORDS (6 TO 12 ENTRIES; ALPHABETICAL ORDER; CAPITALIZE ONLY PROPER NAMES; AND SEPARATE KEY WORDS BY SEMICOLONS)

acoustic emission; composite materials; eddy currents; materials processing; metal forming; nondestructive evaluation; powders ceramic and metal; radiography; sensors; standards; thermal testing; ultrasonics

13. AVAILABILITY

[X] UNLIMITED

[ ] FOR OFFICIAL DISTRIBUTION. DO NOT RELEASE TO NATIONAL TECHNICAL INFORMATION SERVICE (NTIS).

[ ] ORDER FROM SUPERINTENDENT OF DOCUMENTS, U.S. GOVERNMENT PRINTING OFFICE, WASHINGTON, DC 20402.

[X] ORDER FROM NATIONAL TECHNICAL INFORMATION SERVICE (NTIS), SPRINGFIELD, VA 22161.

14. NUMBER OF PRINTED PAGES
80

15. PRICE
A05

ELECTRONIC FORM